

Review

# Skeletal Transformations and the Origin of Baleen Whales (Mammalia, Cetacea, Mysticeti): A Study on Evolutionary Patterns

Michelangelo Bisconti <sup>1,2,\*</sup> and Giorgio Carnevale <sup>1</sup>

<sup>1</sup> Dipartimento di Scienze della Terra, Università degli Studi di Torino, Via Valperga Caluso 35, 10125 Turin, Italy; giorgio.carnevale@unito.it

<sup>2</sup> San Diego Natural History Museum, El Prado 1788, San Diego, CA 92101, USA

\* Correspondence: michelangelo.bisconti@unito.it

**Abstract:** A review of the morphological patterns exhibited by all the main radiations of mysticete (baleen whale) cetaceans provided a broad assessment of the fundamental morphological transformations that occurred in the transition to the Mysticeti clade. Skull and postcranial characters were illustrated, described and compared, and their distribution was mapped on a combined phylogeny in the search for morphological support for the principal mysticete clades (i.e., Mysticeti, Chaemysticeti and Balaenomorpha). In particular, characters of the skull (rostrum, vertex, temporal fossa, tympanic bulla and dentary) and the postcranial appendicular skeleton (scapula, humerus, radius and ulna) were all involved at different degrees in the process of morphological transformations leading to the modern-day mysticetes. Apart from a few typical characteristics of the rostrum that were already present in the earliest-diverging mysticetes (presence of lateral process of the maxilla, presence of multiple dorsal infraorbital foramina, thin lateral border of maxilla and presence of mesorostral groove), most of the other anatomical districts were unaffected by the transition so the earliest mysticetes show a number of archaeocete characters in the tympanic bulla, dentary and skull roof. The analysis of the whole dataset supported the hypothesis that the origin and evolution of mysticetes constituted a step-wise process and that the *bauplan* of the modern-day mysticetes was fully assembled at the level of the common ancestor of all Balaenomorpha.

**Keywords:** character distribution; evolution; fossil record; Mysticeti; paleontology; pattern; phylogeny



**Citation:** Bisconti, M.; Carnevale, G. Skeletal Transformations and the Origin of Baleen Whales (Mammalia, Cetacea, Mysticeti): A Study on Evolutionary Patterns. *Diversity* **2022**, *14*, 221. <https://doi.org/10.3390/d14030221>

Academic Editor: Eric Buffetaut

Received: 7 February 2022

Accepted: 15 March 2022

Published: 18 March 2022

**Publisher's Note:** MDPI stays neutral with regard to jurisdictional claims in published maps and institutional affiliations.



**Copyright:** © 2022 by the authors. Licensee MDPI, Basel, Switzerland. This article is an open access article distributed under the terms and conditions of the Creative Commons Attribution (CC BY) license (<https://creativecommons.org/licenses/by/4.0/>).

## 1. Introduction

Mysticeti or baleen whales are a group of cetaceans including a few extant species in only six genera [1]. Despite their scarce diversity, baleen whales represent key species in the trophic webs of the oceans as they are able to sequester enormous quantities of carbon and to disseminate nutrients that support large planktonic blooms [2–4]. The study of their evolution is thus crucial to understand how and when the ecological characteristics of today's oceans came to be.

It was thought for long time that the origin of baleen whales was related to the origin of those morphological characters that are related to their typical way of feeding: baleen-assisted filter feeding. Different mysticete families use the baleen plates in peculiar ways depending upon their own feeding style [5,6]. However, recent studies have shown that the earliest-diverging mysticetes had skull characters that were remarkably different from those of the extant species, possessed functional dentitions and did not filter feed. The actual origin of the baleen is still not fully understood as the fossil record provides only a few clues on this process, and a cogent debate has developed in the past two decades in the scientific literature on this topic (e.g., [7–10]).

A number of new paleontological discoveries illuminated some aspects of the earliest phases of the evolution of mysticete whales. Late Eocene and Oligocene fossils have helped us to understand part of the transformation process that happened at the origin stage of

Mysticeti, suggesting that the assembly of the mysticete *bauplan* was realized through a step-wise process of character transformation (e.g., [7,11]). However, an extraordinarily limited amount of work has been published dealing with the evolution of characters that are not closely related to feeding in this group. For example, there have been only a few attempts to analyze the origin and evolution of the mysticete forelimb and vertebral column (e.g., [12–14]).

In this work, we attempt to realize an overview of the fundamental morphological transformations that occurred at the origin stage of mysticetes and in concomitance with the origin of the principal mysticete subdivisions. We accept the commonly used name Chaemysticeti [15] to include all the baleen-bearing mysticetes and the name Balaenomorpha [16] to indicate a clade including all the living families of baleen-bearing mysticetes (crown mysticetes). We will discuss morphological evidence related to the diversity of patterns observed in skulls, dentaries, earbones and postcranial skeleton with an emphasis on the forelimb. Then, we will analyze the distribution of the previously discussed morphological characters to infer the character states at ancestral nodes and to understand the principal transformation events occurred in the mysticete phylogeny.

## 2. Materials and Methods

### 2.1. Sources of Comparative Data

We compared anatomical structures from the skull, dentary, earbones, forelimbs and vertebrae from all the published records of the baleen whales. Our taxonomic sample was the same as that published by [17–19] and includes specimens from all the mysticete radiations known to date (Table 1). In addition, we also included *Toipahautea waitaki* [20], *Maiabalaena nesbittae* [21], *Mystacodon selenensis* [22], *Llanocetus denticrenatus* [15] (see also [23]) and *Coronodon havensteini* [10]. Most of the specimens were directly examined by one of us (M. Bisconti), and personal observations were integrated with the information obtained from the relevant literature (cited in [17–19]).

**Table 1.** Stratigraphic ages of the taxa used in the combined phylogeny. Data from Paleobiology Database (<https://paleobiology.org/>, accessed on 23 September 2021) visited on 23 January 2022.

Taxon	Age (Ma)
<i>Cynthiacetus peruvianus</i>	38–33.9
<i>Dorudon atrox</i>	38–33.9
<i>Zygorhiza kochii</i>	38–33.9
Mammalodontidae	27.3–23.03
Aetiocetidae	33.9–25.2
Eomysticetidae	28.4–20.44
Neobalaenidae	11.6–0.0
Balaenidae	23.03–0.0
Cetotheriidae	28.1–2.0
Balaenopteridae	23.03–0.0
Eschrichtiidae	11.6–0.0
<i>Maiabalaena nesbittae</i>	33.9–28.1
<i>Sitsqwayk cornishorum</i>	28.1–23.03
<i>Toipahautea waitaki</i>	34.3–27.3
<i>Llanocetus denticrenatus</i>	38–33.9
<i>Coronodon havensteini</i>	33.9–28.1
<i>Horopeta umarere</i>	27.3–25.2
<i>Pelocetus calvertensis</i>	15.97–13.82
<i>Isanacetus laticephalus</i>	23.03–15.97
<i>Atlantocetus</i>	15.97–13.82
<i>Diorocetus hiatus</i>	15.97–13.82
<i>Parietobalaena palmeri</i>	20.44–13.82
<i>Uranocetus gramensis</i>	11.62–7.246

## 2.2. Anatomy

Anatomical terminology follows that of [24] for skull and dentary with addition of the terms *postcoronoid fossa* and *postcoronoid crest* from [25]. We used [26] for the terminology of the tympanic bulla and periotic. The characters discussed in the text are shown in Figures 1–3. In Figure 1, the skull of *Dorudon atrox* (modified from [27]) and that of *Balaenoptera physalus* (modified from [28]) are shown with indications of most of the skull characters discussed in the text. Since *Dorudon atrox* is an archaeocete, it illustrates the plesiomorphic characters that were presumably present in mysticete ancestors. In Figure 2, the tympanic bullae of *Dorudon atrox* and *Atlantictetus patulus* (redrawn from [29]) are shown to illustrate the schematic code used in the comparative analysis. These bullae were selected to illustrate the presence (*Atlantictetus patulus*) and absence (*Dorudon atrox*) of the anterior lobe. In Figure 3, the dentaries of *Dorudon atrox* and *Balaenoptera physalus* are shown to indicate the morphological characters. In Figure 4, the skeleton of the forelimb (with the exclusion of the *manus*) of *Zygorhiza kochii*, a dorudontine archaeocete, is shown with indications of morphological characters.

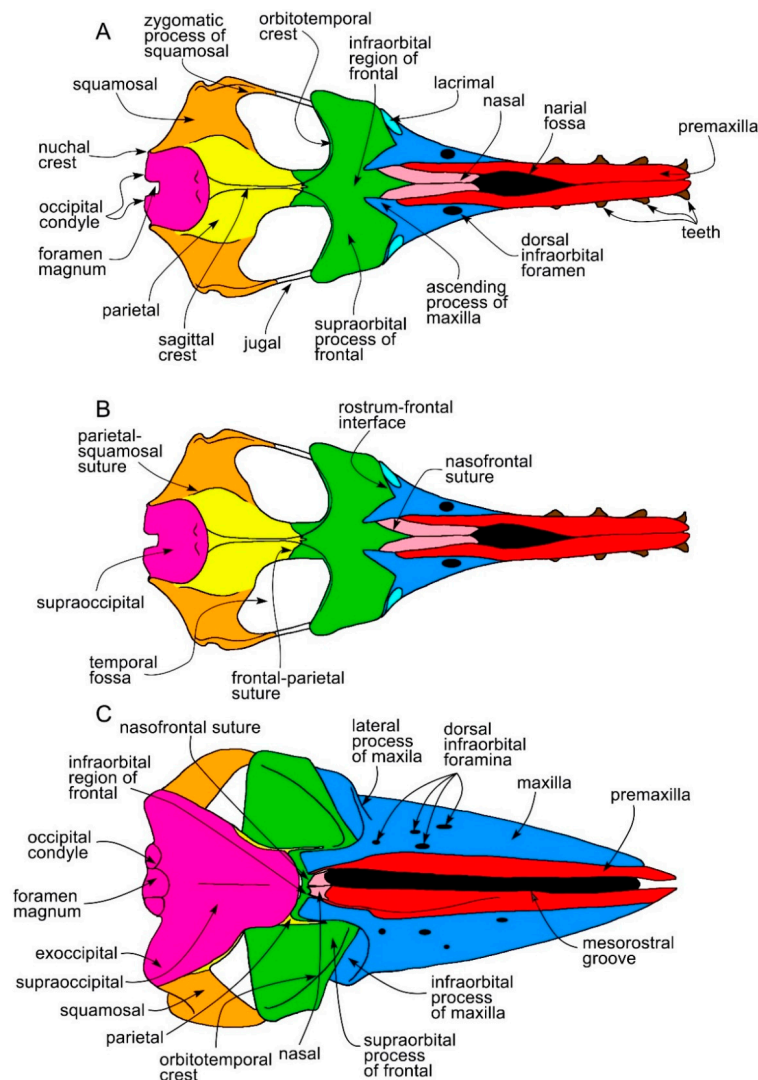


**Figure 1.** Osteological characters discussed in the text. (A) Skull of *Dorudon atrox* in dorsal view showing the bones forming the cranial vault and the rostrum. (B) Skull of *Dorudon atrox* in dorsal view showing sutures and additional structures. (C) Skull of *Balaenoptera physalus* in dorsal view showing the bones forming the cranial vault, the rostrum and peculiar characteristics of the mysticete skull. Not to scale. The skulls were drawn as if they shared the same condylobasal length.

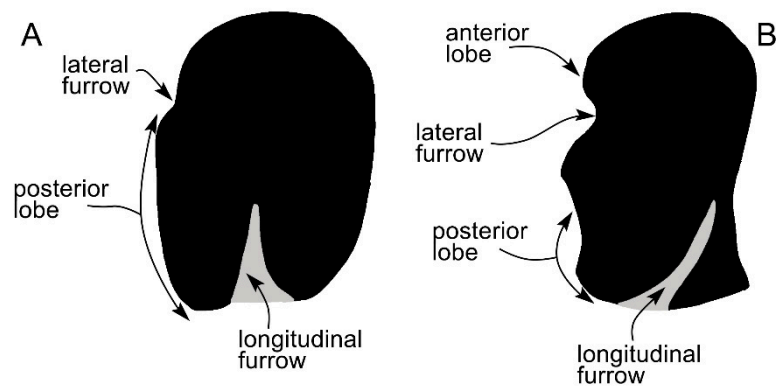


**Figure 2.** Schematic representations of tympanic bullae in ventral view showing characters discussed in the text. (A) Tympanic bulla of *Dorudon atrox*; note the absence of the anterior lobe. (B) Tympanic bulla of *Atlantictetus patulus*; note the presence of the anterior lobe. Not to scale. The bullae were drawn as if they shared the same anteroposterior length.

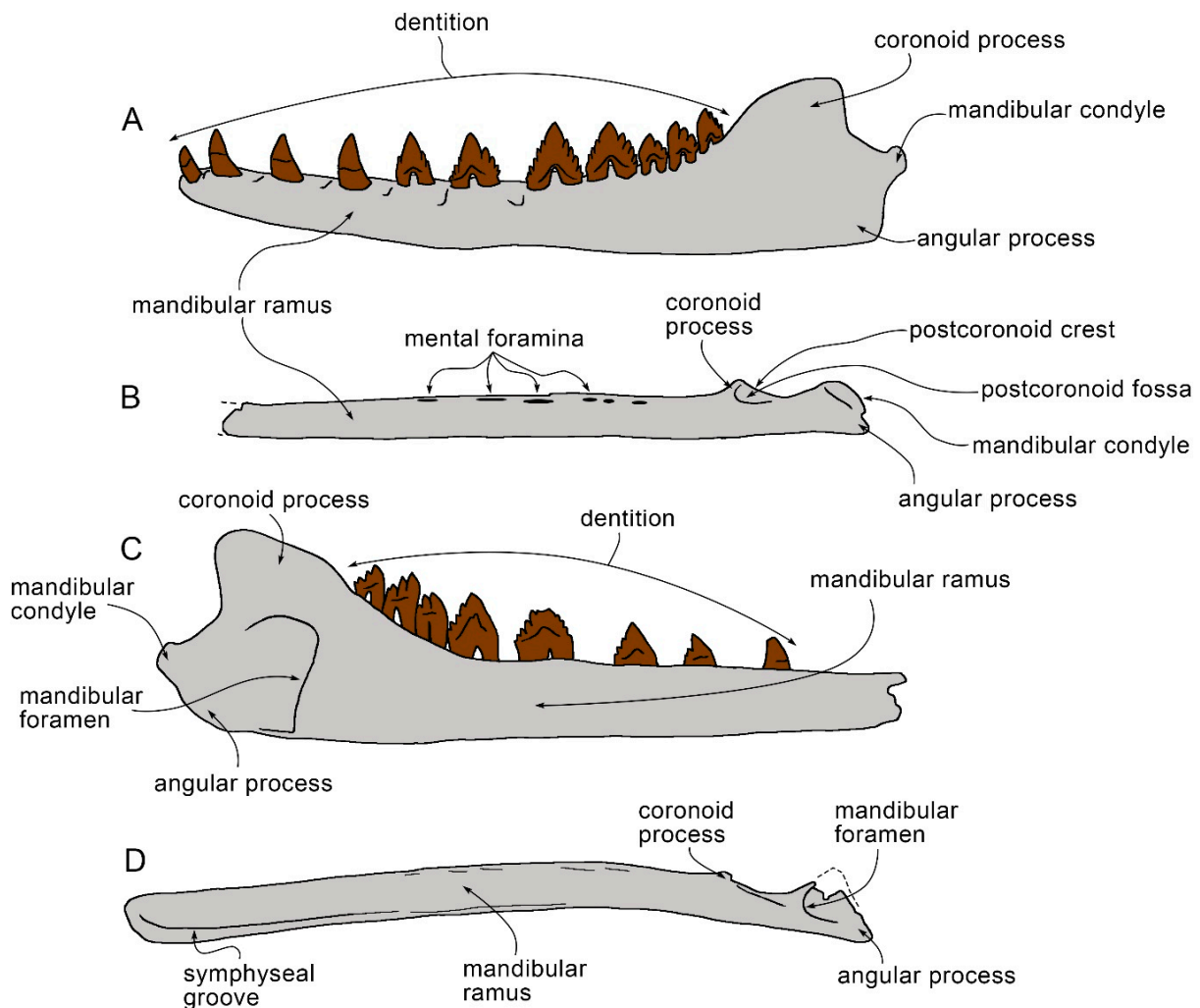


**Figure 3.** Schematic representation of the dentary of an archaeocete and a mysticete showing characters discussed in the text. (A) *Dorudon atrox*, dentary in lateral view. (B) *Herpetocetus morrowi*, dentary in lateral view. (C) *Dorudon atrox*, dentary in medial view. (D) *Herpetocetus morrowi*, dentary in medial view. Not to scale. The dentaries are represented as if they shared the same anteroposterior length. Representations of mysticete dentaries follows the conventional rules described in [17].

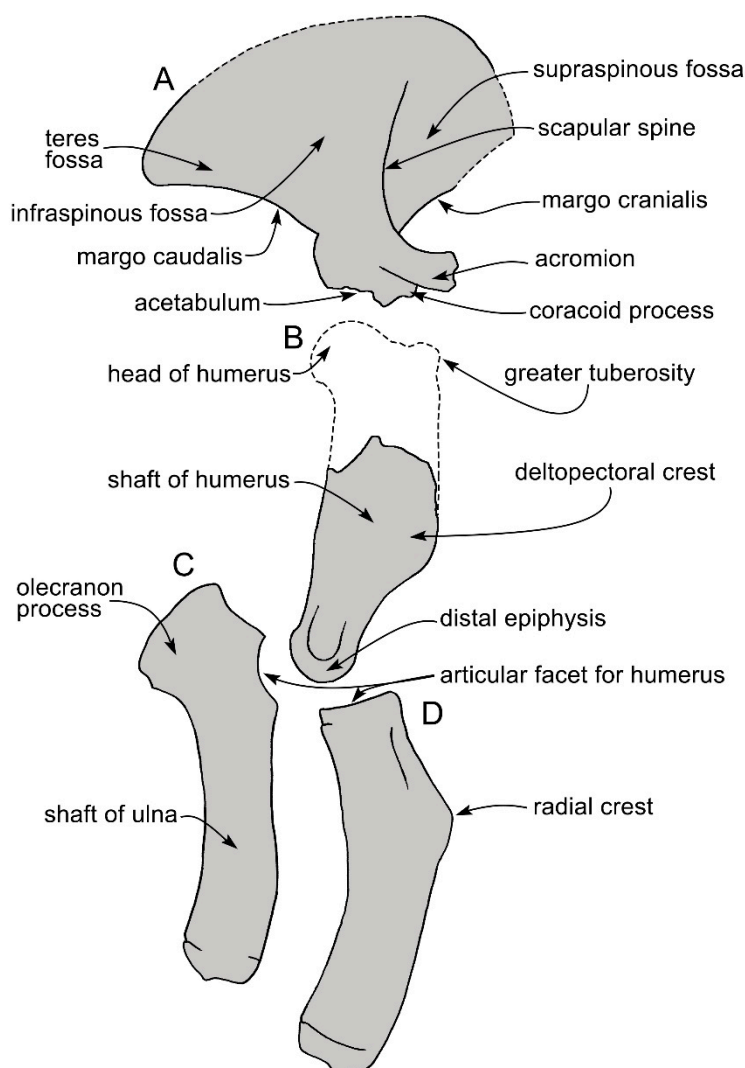


**Figure 4.** Schematic representation of the appendicular skeleton of *Zygorhiza kochii* (United States National Museum, Smithsonian Institution No. 4673; specimen mirrored in the present figure) in lateral view showing characters discussed in the text. (A) Scapula. (B) Humerus. (C) Ulna. (D) Radius. Not to scale.

### 2.3. Phylogeny

We assembled a hypothesis of phylogenetic relationships among mysticetes based on several sources (Figure 5), as detailed in the following text. The phylogeny in Figure 5 mainly relies on the general structure of the mysticete phylogeny as derived from the works of [17–19,30–33], in which Mysticeti, Chaemysticeti, Balaenomorpha, Balaenoidea, Thalassotheerii and Balaenopteroidea represent monophyletic clades. The monophyly of Mysticeti, Chaemysticeti, Balaenoidea and Balaenomorpha is also supported by several morphology- and total-evidence-based works (e.g., [7,21,34–39]). The monophyly of Balaenoidea (including Neobalaenidae and Balaenidae) is also supported by, e.g., [21,35–37] (morphological partition only) and [39–45]. Further support for the monophyly of the basal thalassotheerian taxa (including *Parietobalaena*, *Pelocetus*, *Atlantictetus* and *Uranocetus*) is provided by [21,35,40–42,46]. The sister group relationship of Cetotheriidae and Balaenopteroidea (including Eschrichtiidae and Balaenopteridae) is supported by [34,40–42,47] (analysis under implied weighting). In Figure 6, the branching pattern of representative taxa within single families is illustrated mainly on the basis of the phylogenetic results of [17–19,30]. In Figure 7, the branching pattern of the composite phylogeny is plotted against a geological time scale to show the stratigraphic distribution of the taxa.

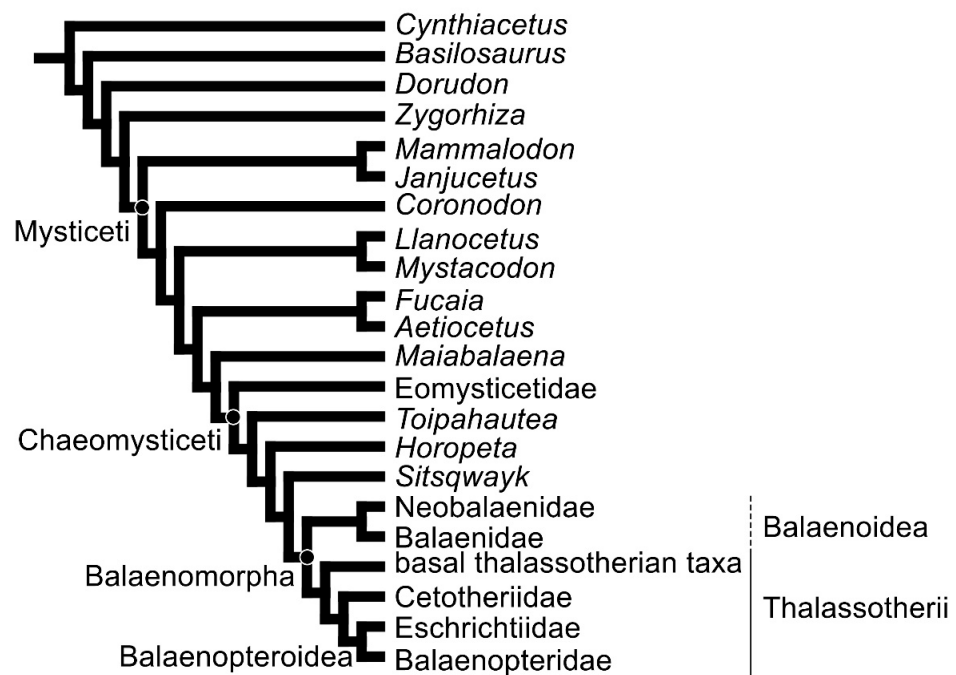


**Figure 5.** Phylogenetic relationships among the main mysticete clades used in this paper. The three named, high-rank clades Mysticeti, Chaemysticeti and Balaenomorpha are circled. Relationships among superfamilies (Balaenoidea and Thalassotherii), one epifamily (Balaenopteroidea) and families are shown.

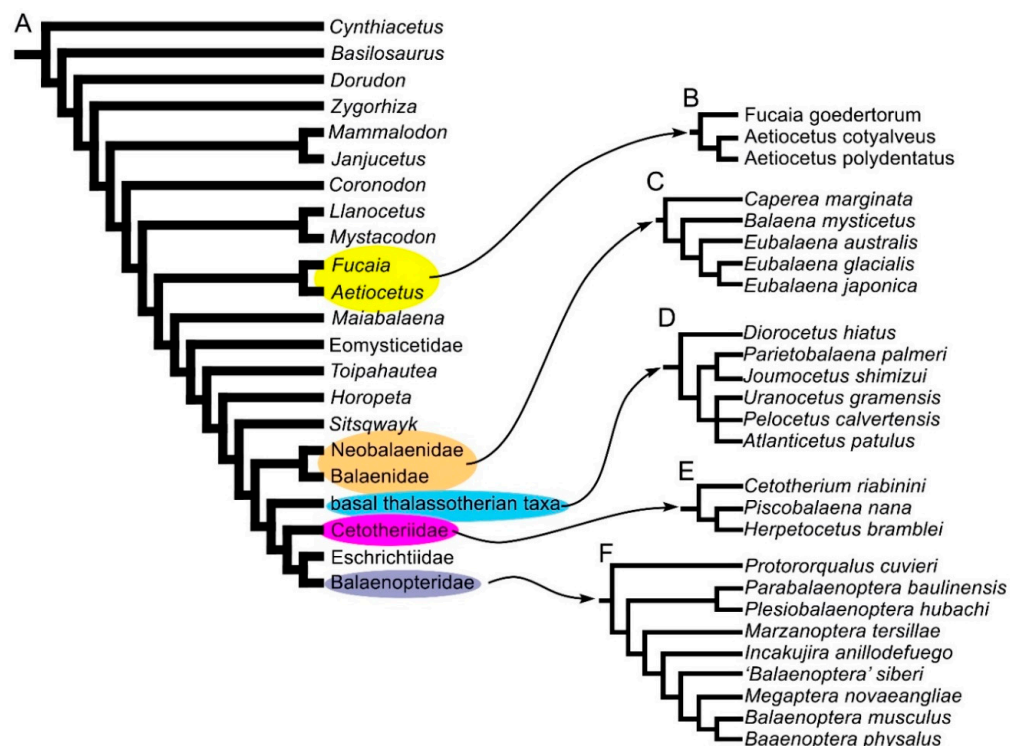


**Figure 6.** Intrafamily relationships among most of the mysticete species discussed in the text. The shown taxa are discussed in the present paper. (A) consensus phylogeny of Mysticeti adopted in the present paper. (B) relationships of aetiocetid taxa. (C) phylogenetic relationships of Balaenoidea. (D) relationships of basal thalassotherian taxa. (E) relationships of Cetotheriidae. (F) phylogenetic relationships of Balaenopteridae.

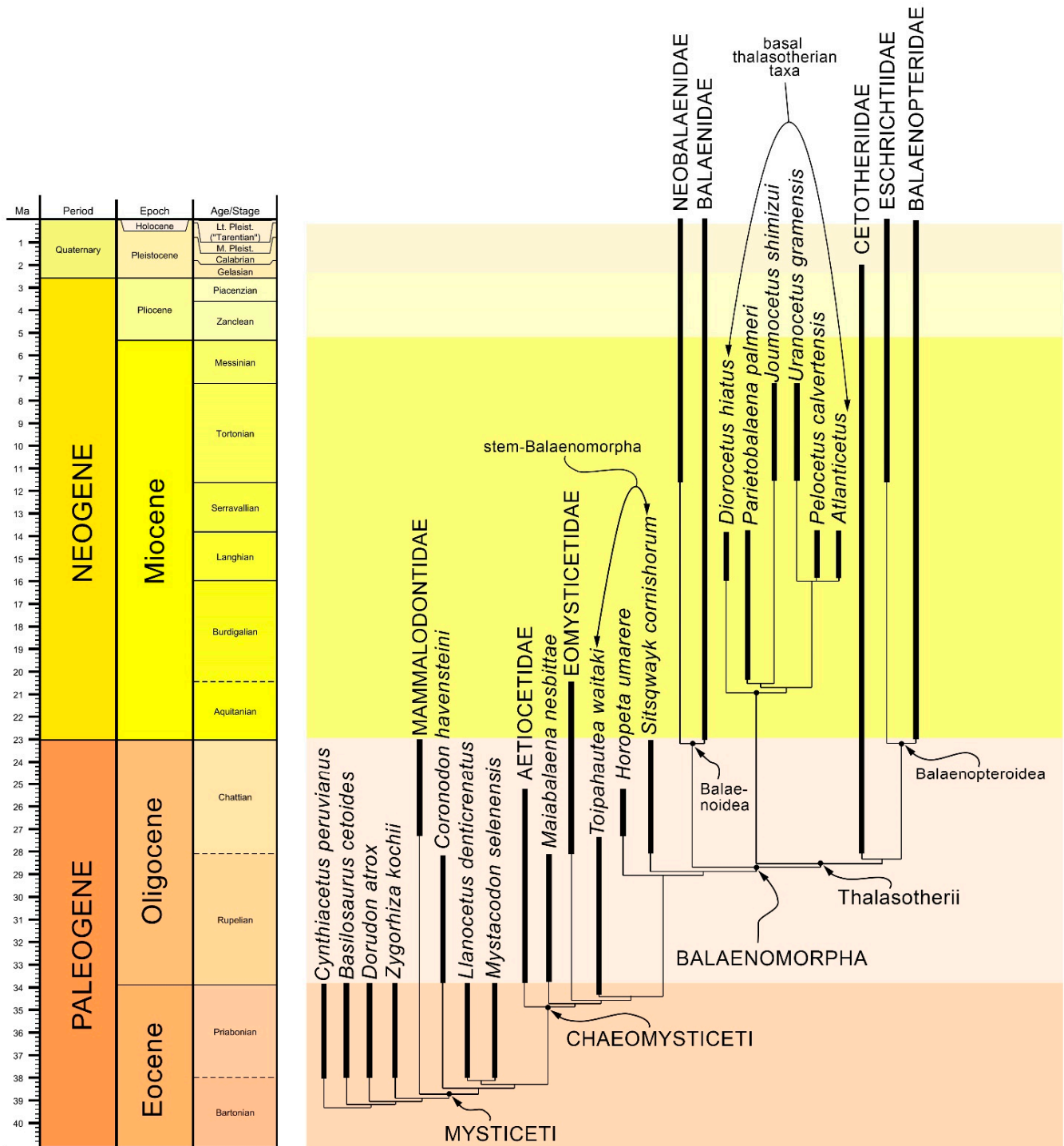


**Figure 7.** Stratigraphic distributions of the mysticete clades discussed in this paper. The geologic scale chart was produced with TSCreator (<https://engineering.purdue.edu/Stratigraphy/tcreator>, accessed on 17 July 2020).

#### 2.4. Character Mapping and Reconstruction of Characters at Ancestral Nodes

The distributions of the morphological characters discussed in the text were coded for cladistic analysis (Table 2) and used to compile a character x taxon matrix (Table 3). The matrix was treated with MESQUITE 3.6 [48] by using the maximum likelihood algorithm as implemented in the software with Mk1 model of character distribution to infer character evolution and to reconstruct character states at ancestral nodes.

**Table 2.** Character states used in the analysis of character distribution.

	Character	State 0	State 1
Rostrum			
1	Lateral process of maxilla	Absent	Present
2	Infraorbital plate	Absent	Present
3	Dorsal infraorbital foramina	Single	Multiple
4	Mesorostral groove	Absent	Present
5	Border of maxilla	Thick	Thin
6	Teeth on maxilla, premaxilla, dentary	Present	Absent
7	Position of anterior border of nasal with respect to total maxillary length	In the anterior half	In the posterior half
Vertex			
8	Position of nasofrontal suture	Anterior border of interorbital region of frontal	Within interorbital region of frontal
9	Ascending process of maxilla	Short (length < 5 times width)	Long (length > 5 times width)
10	Supraoccipital superimposed on interorbital region of frontal	no	Yes
11	Parietal exposure at vertex	Long (posterior border in the posterior half of temporal fossa)	Short (posterior border in the anterior half of temporal fossa)
12	Sagittal crest	Acute	Double and flat
Temporal fossa			
13	Orbitotemporal crest location	Posterodorsal edge of supraorbital process of frontal	Diagonal on supraorbital process of frontal (with variations)
14	Nuchal crest posterior to occipital condyles	Yes	No
15	Intertemporal constriction	Narrow	Wide
16	Intertemporal constriction	Long	Short
Occipital region			
17	Supraoccipital orientation	More vertical	More horizontal
18	Posterior transverse constriction of occipital region at level of nuchal crest	Present	Absent
Tympanic bulla			
19	Anterior lobe	Absent	Present
20	Ventral furrow	Short	Long
<i>Dentary</i>			
21	Comparative length of ramus	Short	Long
22	Height of coronoid process	High	Low
23	Orientation of coronoid process	In line with ramus	Deflected
24	Symphyseal groove	Absent	Present
Appendicular skeleton			
25	Orientation of margo caudalis of scapula	About 50°	About 30°
26	Supraspinous fossa of scapula	Wide	Narrow
27	Greater tubercle of humerus	Well-developed	Reduced
28	Deltpectoral crest of humerus	Well-developed and long	Reduced-to-absent
29	Radial crest of radius	Present	Absent
30	Articulation between humerus, radius and ulna	Rotational	Nonrotational
31	Angle below olecranon	Wide and curve	Acute

**Table 3.** Character x taxon matrix used in the analysis of character distribution and inference of character states at ancestral nodes.

<i>Cynthiacetus peruvianus</i>	00000000000000000000000000000000
<i>Basilosaurus cetoides</i>	00000000000000000000000000000000
<i>Dorudon atrox</i>	00000000000000000000000000000000
<i>Zygorhiza kochii</i>	00000000000000000000000000000000
Mammalodontidae	1111000000001001100000???????
<i>Coronodon havensteini</i>	1111100000001001100???????????
<i>Llanocetus denticrenatus</i>	1111100000001001100?000???????
<i>Mystacodon selenensis</i>	1111100000001001100100000????10
<i>Fucaia goedertorum</i>	11111000000010011001101???????
<i>Aetiocetus cotylalveus</i>	11111000000010011001101???????
<i>Aetiocetus polydentatus</i>	111110110000010011001101???????
<i>Maiabalaena nesbittae</i>	11111000000010011001101?00???
Eomysticetidae	111111000000100110011011000111
<i>Toipahautea waitaki</i>	111111?????0?001100?101???????
<i>Horopeta amarere</i>	111111?????0?001100?11101?111
<i>Sitsqwayk cornishorum</i>	111111000000100110011111000111
Neobalaenidae	1111111000--1111111111-11111111
Balaenidae	1111111000--1111111111-101111110
<i>Diorocetus hiatus</i>	111111100110111111001111????111
<i>Parietobalaena palmeri</i>	111111100010111111001111???????
<i>Joumocetus shimizui</i>	111111100010111111001111???????
<i>Pelocetus calvertensis</i>	1111111000101011111011110111?11
<i>Atlantocetus patulus</i>	111111100010101111101111???????
<i>Uranocetus gramensis</i>	111111100010101111101111?11?11
Cetotheriidae	11111111101100111100111111111111
Eschrichtiidae	11111111101110111110111101111111
Balaenopteridae	1111111110-11111111011111111111

### 3. Results

#### 3.1. Rostrum

In the earliest-diverging mysticetes, i.e., Mammalodontidae, the rostrum is short and the neurocranium represents a higher portion of the skull length (Figure 8). However, differing from archaeocetes, in *Mammalodon* and *Janjucetus*, the dorsal infraorbital foramen is represented by a cluster of foramina located in the posterior portion of the maxilla. The dorsal infraorbital foramen provides the maxillary ramus of the trigeminal nerve a path through the maxilla from the endocranial cavity where it is represented by a robust, bilateral nerve trunk in both the Odontoceti and Mysticeti ([49,50] and literature therein). In the Mammalodontidae, the frontal-rostrum articulation is reduced to the ascending processes of the maxilla and premaxilla, the latter being transversely and anteroposteriorly reduced. The posterolateral border of the maxilla produces a short and narrow lateral process and a flattened infraorbital process developed ventrally to the supraorbital process of the frontal. Anteriorly to the nasal, the narial fossa is prolonged anteriorly and forms a mesorostral groove. Most of the rostral characters of balaenomorph mysticetes were already present in the earliest-diverging mysticetes known up to now, the Mammalodontidae, in

which the rostrum lacks the strong elongation observed in the later-diverging branches (e.g., Aetiocetidae, Eomysticetidae and so on).

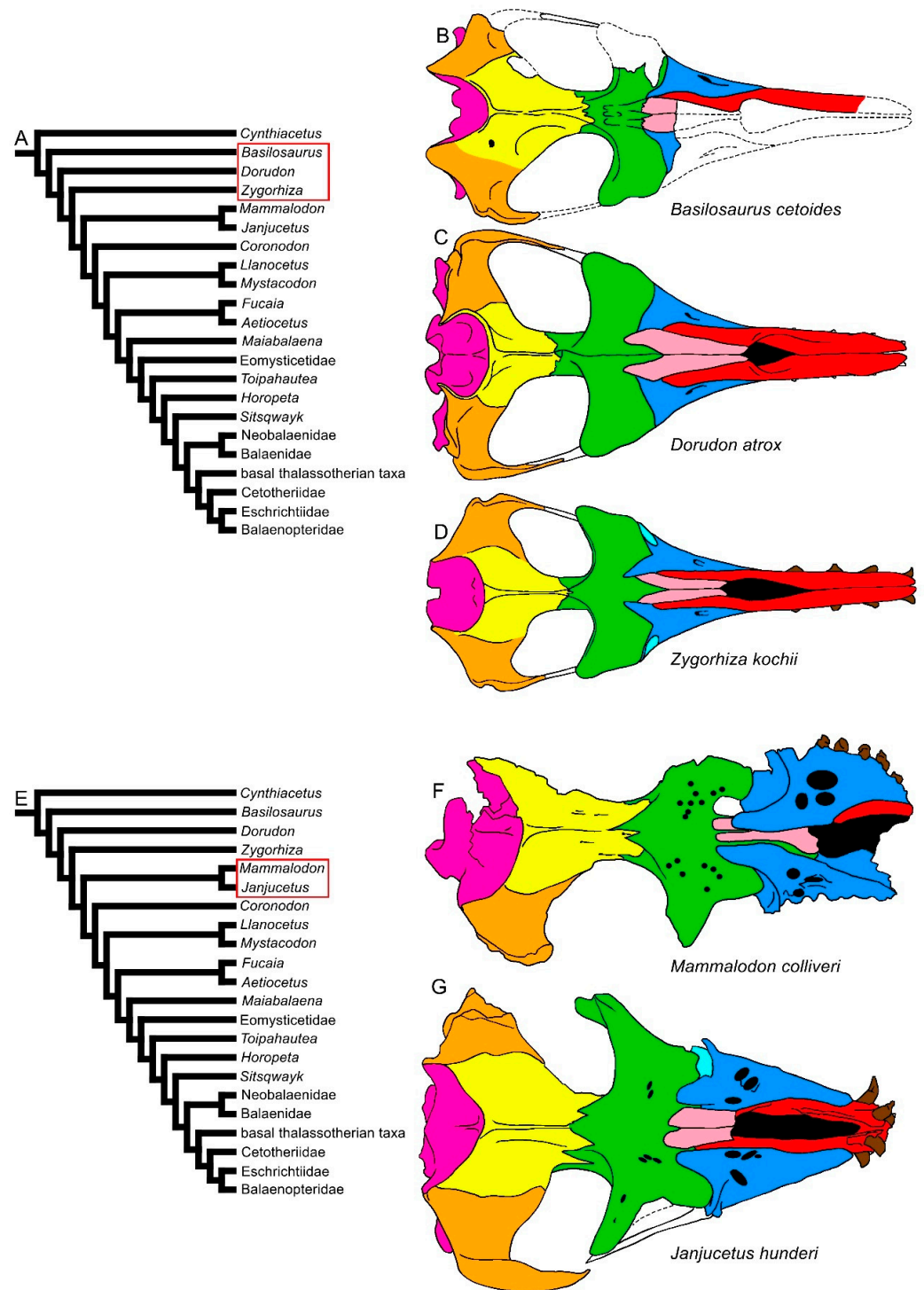


**Figure 8.** Diversity of the skull in dorsal view in basilosaurine and dorudontine archaeocetes and in mysticetes. (A) Phylogenetic relationships among archaeocetes and mysticetes showing the archaeocete branching (red ellipsis). (B) Skull of *Basilosaurus cetoides*. (C) Skull of *Dorudon atrox*. (D) Skull of *Zygorhiza kochii*. (E) Phylogenetic relationships among archeocetes and mysticetes showing the ramus leading to Mammalodontidae (red ellipsis). (F) Skull of *Mammalodon colliveri*. (G) Skull of *Janjucetus hunderi*. Not to scale. The skulls are represented as if they shared the same condylobasal length.

The subsequent branches are represented by the Oligocene *Coronodon havensteini*, *Llanocetus denticrenatus* and *Mystacodon selenensis* (Figure 9). In these taxa, the rostrum is longer compared to that of Mammalodontidae. *Mystacodon* shows an archaeocete-like rostrum in that the mesorostral groove is short and the maxilla is transversely shortened, giving the rostrum a narrow and pointed shape that resembles that observed in *Dorudon*, *Cynthiacetus*, *Basilosaurus* and *Zygorhiza* (compare Figures 8 and 9A–D). In both *Coronodon* and *Mystacodon*, the rostrum represents about half of the whole skull length. In *Coronodon*, moreover, the lateral borders of the maxilla are thin as in more recent mysticetes.

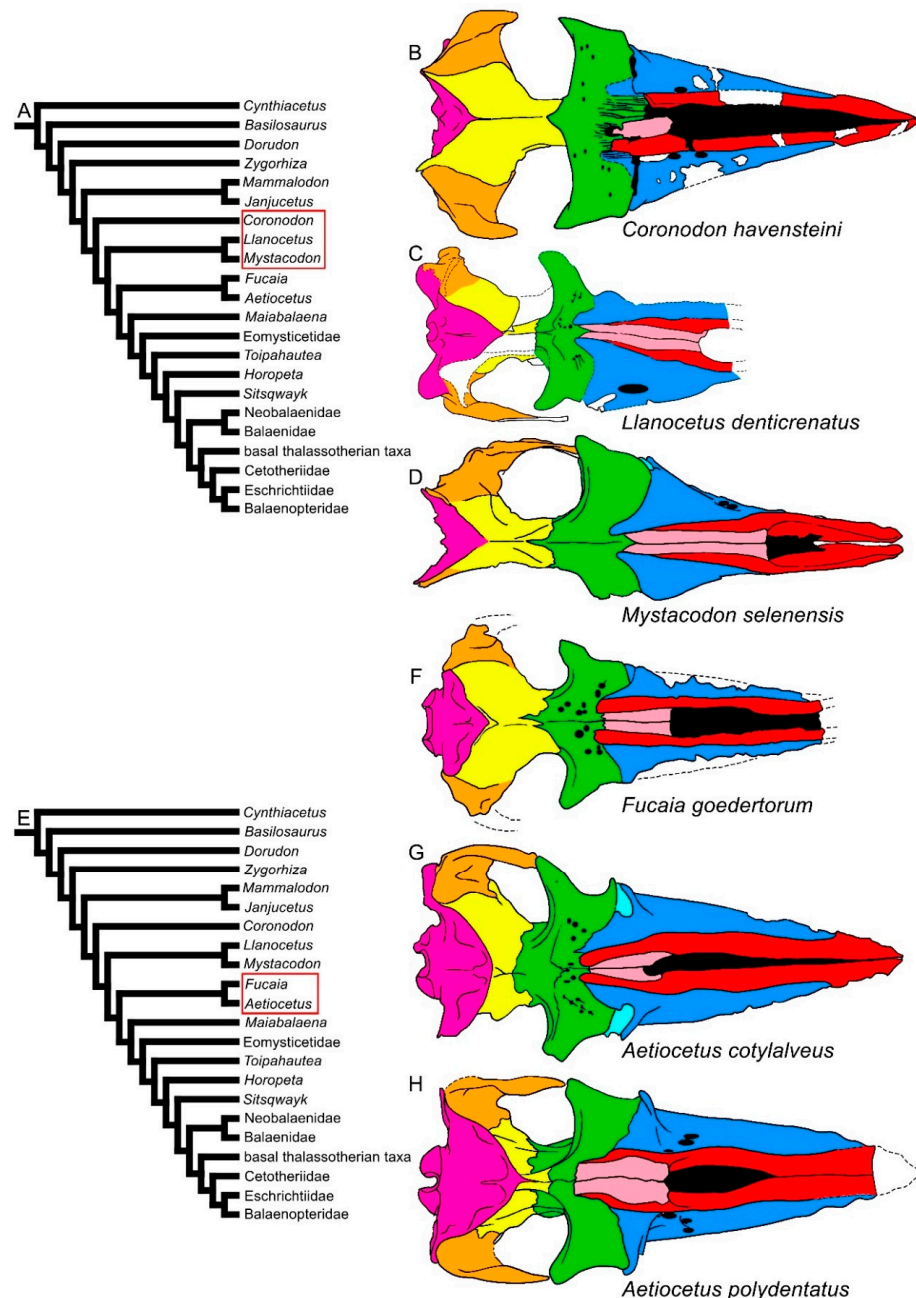


**Figure 9.** Diversity of mysticete skulls in dorsal view. (A) Phylogenetic relationships among mysticetes showing the branching order of *Coronodon*, *Llanocetus* and *Mystacodon* (red ellipsis). (B) Skull of *Coronodon havensteini*. (C) Skull of *Llanocetus denticrenatus*. (D) Skull of *Mystacodon selenensis*. (E) Phylogenetic relationships among mysticetes showing the branching order of *Fucaia* and *Aetiocetus* (red ellipsis). (F) Skull of *Fucaia goedertorum*. (G) Skull of *Aetiocetus cotylalveus*. (H) Skull of *Aetiocetus polydentatus*. Not to scale. The skulls are represented as if they shared the same condylobasal length.

In the clade formed by *Fucaia* and *Aetiocetus* (corresponding to the Aetiocetidae family), the rostrum is transversely expanded, and its external outline is externally convex, resembling that of most Chaecomysticeti (Figure 9E–H). The elongation of the rostrum remarkably increases in the Eomysticetidae (Figure 10C–E), while it continues to represent about the half of the skull length in *Maiabalaena* and *Sitsqwayk* (Figure 10A,F). In the Eomysticetidae, the rostrum represents about 60% of the whole skull length, shows a border that is thin and externally convex, and a broadly expanded maxilla. The nasal is elongated and reaches c. 30% of the rostrum length. Interestingly, the nasal bone diminishes in proportional length independently in different clades. For example, in *Mystacodon*, *Maiabalaena* and *Sitsqwayk*, the nasal length is about 50% of the rostrum length, but in Aetiocetidae the nasal length is about 20% of such a length. Nasal reduction occurred independently in different mysticete clades.

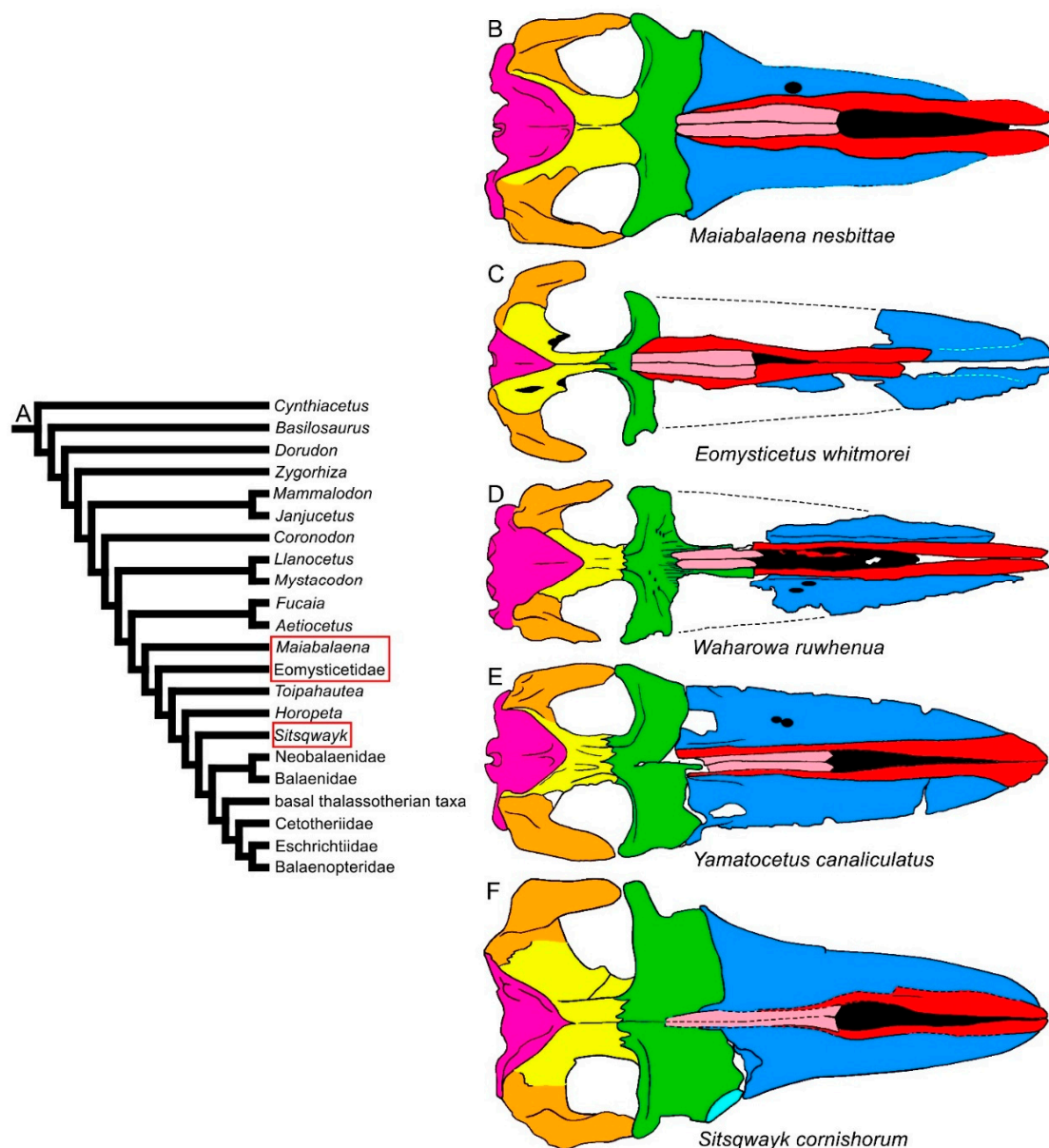


**Figure 10.** Diversity of mysticete skulls in dorsal view: stem- and early Chaecomysticeti. (A) Phylogenetic relationships among mysticetes showing the branching order of *Maiabalaena*, Eomysticetidae and *Sitsqwayk* (red ellipses). (B) Skull of *Maiabalaena nesbittae*. (C) Skull of *Eomysticetus whitmorei*. (D) Skull of *Waharowa ruwhenua*. (E) Skull of *Yamatocetus canaliculatus*. (F) Skull of *Sitsqwayk cornishorum*. Not to scale. The skulls are represented as if they shared the same condylobasal length.

Within the Chaecomysticeti, the diversity of the rostrum increases in terms of transverse expansion and articulation patterns with the frontal. In Balaenoidea, two distinct patterns are observed: one is that of the Neobalaenidae, in which the rostrum is transversely expanded and greatly arched dorsoventrally [43]; the ascending process of the maxilla is reduced to a squared posteromedial projection. The other is that of the Balaenidae, in which the ascending process of the maxilla may be wide and posteriorly pointed or squared and short, and the maxilla is transversely narrowed, showing lateral borders parallel to the longitudinal axis of the skull (Figure 11). The balaenid rostra are strongly arched along the dorsoventral axis like that of the Neobalaenidae. Compared to the mysticetes in which the rostrum is mostly horizontal, the space between the ventral surface of the rostrum and the floor of the mouth cavity is massively enlarged in the Balaenoidea, and this allows the allocation of a large and muscular tongue and up to 4 m-long baleen plates [6]. In both the Balaenidae and Neobalaenidae, the squamosal is elongated dorsoventrally, and the craniomandibular joint is comparatively more ventral than in the other baleen-bearing mysticetes [51,52]. Both these families mainly filter feed upon calanoid copepods and share a number of feeding-related morphological characters (e.g., reduced coronoid process of the dentary, presence of mylohyoidal groove in the dentary and elongated baleen).

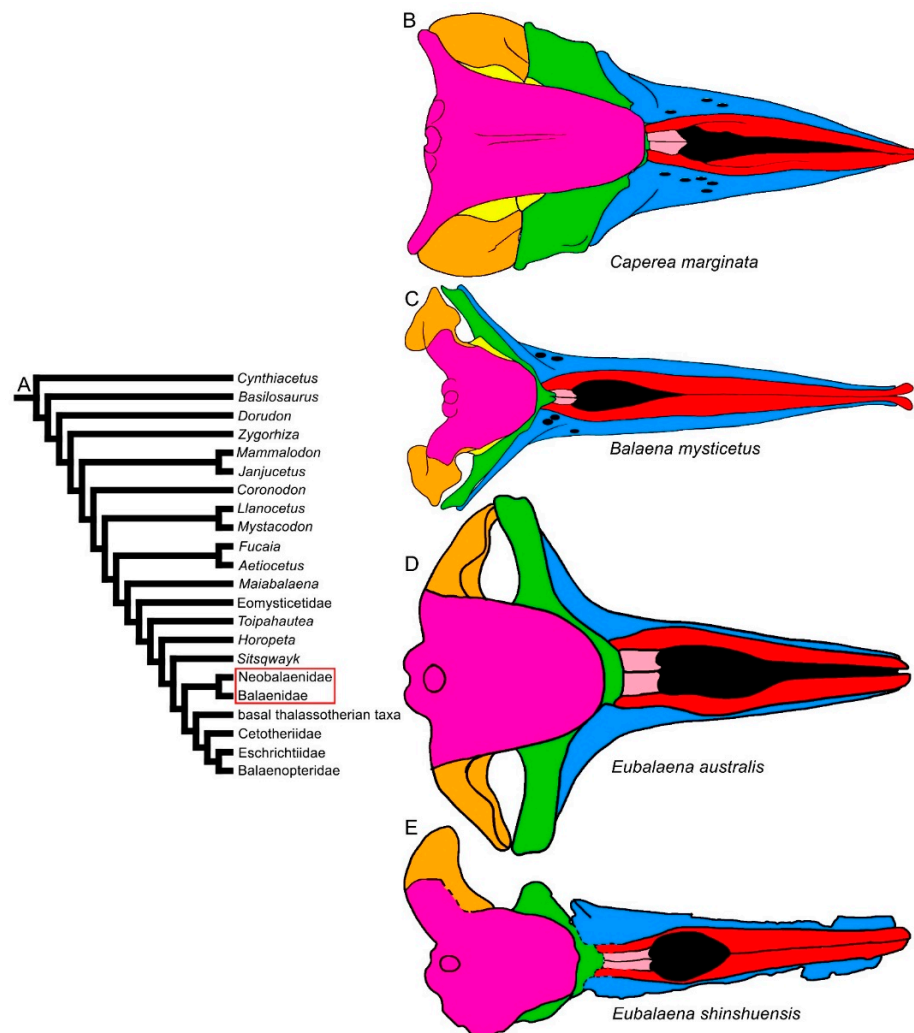


**Figure 11.** Diversity of balaenomorph mysticete skulls in dorsal view: Balaenoidea. (A) Phylogenetic relationships among mysticetes showing the branching order of Balaenoidea. (B) Skull of *Caperea marginata*. (C) Skull of *Balaena mysticetus*. (D) Skull of *Eubalaena australis*. (E) Skull of *Eubalaena shinshuensis*. Not to scale. The skulls are represented as if they shared the same condylobasal length.

The superfamily *Thalassotheri* is characterized by four families in which the rostrum is mainly horizontal and flat. The gray whales, *Eschrichtiidae*, are the only group within this superfamily in which the rostrum is arched in at least one species (i.e., *Eschrichtius robustus*). Two different patterns of articulation between rostrum and frontal are observed: (1) in the basal thalassotherian taxa, the ascending process of the maxilla is short, wide and posteriorly pointed resembling that of *Eubalaena glacialis* (Figure 12); and (2) in the *Cetotheriidae* and *Balaenopteroidea*, the ascending process of the maxilla is much more elongated and narrow (Figures 13 and 14). These two patterns are related to the different shapes of the parietal-frontal suture that is anteriorly convex in dorsal view in the basal thalassotherian taxa and anteriorly concave in most *Cetotheriidae* and *Balaenopteroidea*. The length of the ascending process of the maxilla is especially increased in a number of cetotheriid (e.g., *Piscobalaena nana*, *Herentalia nigra* and *Tranotocetus maregermanicum*) and balaenopterid taxa (e.g., all the balaenopterid genera with the exception of '*Balaenoptera*' *ryani* and '*Balaenoptera*' *cortesii* var. *portisi*), so that the parietal interdigitates with it [34,53–57].

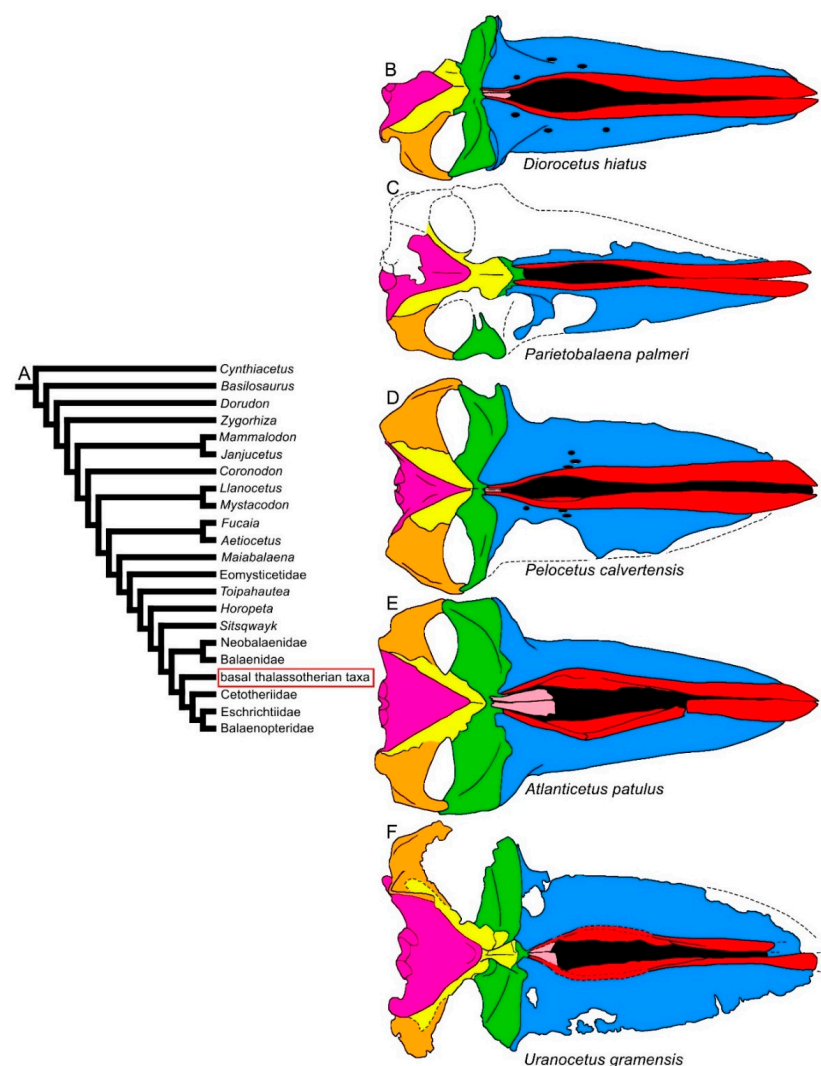


**Figure 12.** Diversity of balaenomorph mysticete skulls in dorsal view: basal thalassotherian taxa. (A) Phylogenetic relationships among mysticetes showing the branching order of the basal thalassotherian clade. (B) Skull of *Diorocetus hiatus*. (C) Skull of *Parietobalaena palmeri* (United States National Museum, Smithsonian Institution No. 10677). (D) Skull of *Pelocetus calvertensis*. (E) Skull of *Atlanticeetus patulus*. (F) Skull of *Uranocetus gramensis*. Not to scale. The skulls are represented as if they shared the same condylobasal length.

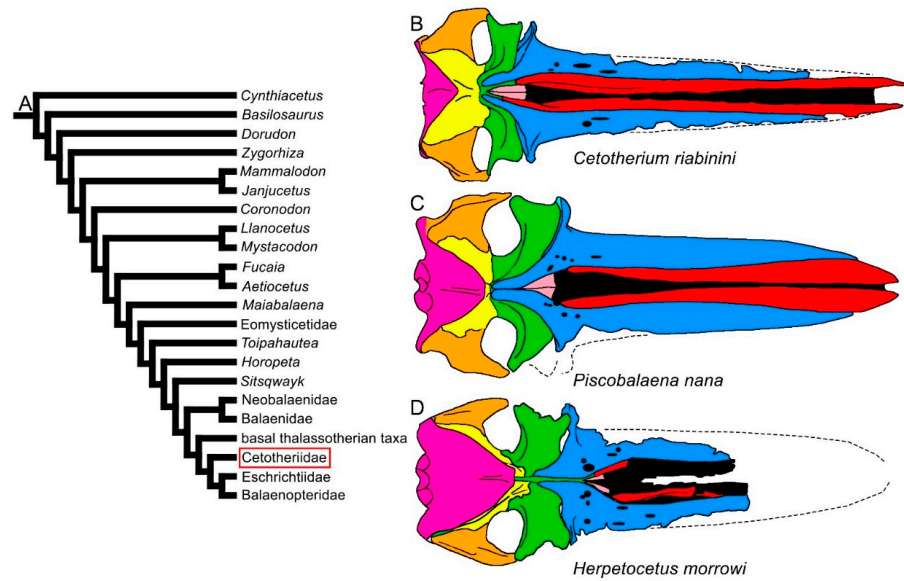


**Figure 13.** Diversity of balaenomorph mysticete skulls in dorsal view: Cetotheriidae. (A) Phylogenetic relationships among mysticetes showing the position of Cetotheriidae. (B) Skull of *Cetotherium riabinini*. (C) Skull of *Piscobalaena nana*. (D) Skull of *Herpetocetus morrowi*. Not to scale. The skulls are represented as if they shared the same condylobasal length.

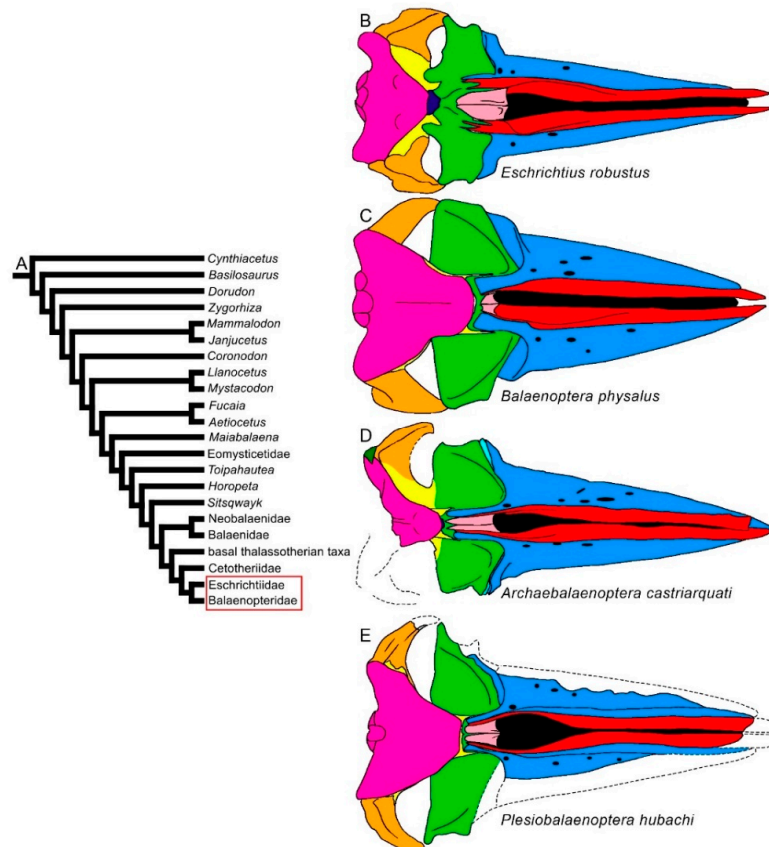


**Figure 14.** Diversity of balaenomorph mysticete skulls in dorsal view: Balaenopteroidea. (A) Phylogenetic relationships among mysticetes showing the position of Balaenopteroidea (Eschrichtiidae and Balaenopteridae). (B) Skull of *Eschrichtius robustus*. (C) Skull of *Balaenoptera physalus*. (D) *Archeobalaenoptera castriarquati*. (E) *Plesiobalaenoptera hubachi*. Not to scale. The skulls are represented as if they shared the same condylobasal length.

The transverse width of the rostrum may be highly diverse within the Thalassotheriia. In basal thalassotherian taxa, it is possible to recognize two groups (based on the phylogenetic results of [17–19,30]): one in which the rostrum width is particularly expanded (including *Atlantocetus patulus*, *Pelocetus calvertensis*, *Isanacetus laticephalus* and *Uranocetus gramensis*) and another in which the rostrum is comparatively narrower (including *Diorocetus hiatus*, *Parietobalaena palmeri*, *P. campiniana* and *P. yamaokai*) (see differences shown in Figure 12). A wide rostrum is related to an increased gape, suggesting that feeding adaptations were finely modulated within this monophyletic group. The same pattern is observed within the Balaenopteridae, in which broad-nosed and sharp-nosed species are observed within the same genera. Examples are the sharp-nosed *Balaenoptera acutorostrata* and *Balaenoptera physalus* and the broad-nosed *Balaenoptera musculus*; additional examples are the sharp-nosed *Archaeobalaenoptera castriarquati* and the broad-nosed *Archaeobalaenoptera eusebioi* [58,59]. The differences that can be observed in the rostrum of cetotheriids (compare, for example, the narrow rostrum of *Cetotherium riabinini* and the broader rostrum of *Piscobalaena nana* and *Herpetocetus morrowi* in Figure 13) may be related to similar functional differences, suggesting that different feeding adaptations were present in this extinct family. Additional work is still needed, however, to determine the fine differences in the rostra of these taxa.

Long nasal bones are present in early-diverging balaenopterids, such as *Archaeobalaenoptera castriarquati* and *Parabalaenoptera baulinensis* [51,60], although the nasal bones are strongly reduced in both length and width in all the other Balaenomorpha. In the Cetotheriidae and Balaenopteroidea, most of the taxa show the nasofrontal suture located well within the interorbital region of the frontal, a character not observed in the Balaenoidea and basal thalassotherian taxa. In Aetiocetidae, the same trend is observed as the nasofrontal suture is located at the anterior border of the interorbital region of the frontal in *Fucaia* and *Aetiocetus cotylalveus* but it is located within the interorbital region of the frontal in *Aetiocetus polydentatus*.

In conclusion, the examination of the morphological diversity of the rostrum in the fossil record of baleen whales shows that the earliest mysticetes were equipped with most of the morphological characters observed in later-diverging clades (articulation between rostrum and frontal provided by the ascending process of the maxilla and premaxilla, presence of mesorostral groove, lateral process of the maxilla, infraorbital process of the maxilla and multiple dorsal maxillary foramina). The rostrum-length-to-skull-length ratio increased in early mysticetes but only in the Eomysticetidae is the rostrum markedly longer than the neurocranium, a character present in all Balaenomorpha probably related to a peramorphic process as discussed by [40–42]. Rostrum diversity expands to Balaenomorpha, where different patterns of articulation between rostrum and frontal and different maxillary and premaxillary morphologies are observed, possibly related to different feeding strategies [5].

### 3.2. Vertex

According to ([24], p. 155), “The vertex has assumed a new role in the cetacean skull as a result of the posterior movement of the external nares. The vertex in terrestrial mammals was a craniometric point, defined as the most dorsal point on the skull, and did not have a definite function. In cetaceans [ . . . ] it serves as a nexus for many groups of muscles. The vertex serves as a foundation on which the muscles that control the movements of the nasal passage and associated diverticula rely. The vertex is primarily centered on the nasal bones. In groups in which the vertex is more highly developed, [ . . . ] the vertex consists of the nasals and surrounding portions of the maxillae, premaxillae, and frontals.”

Comparative illustrations of the mysticete vertex have been provided by [59] for the balaenopterid genus *Archaeobalaenoptera*, [61] for Cetotheriidae, [43] for the neobalaenid *Caperea* and *Miocaperea* [62] and for some species of extant *Balaenoptera*. Additional observations can be made based on Figures 8–14 of the present paper.

Early-diverging mysticetes (i.e., Mammalodontidae, Aetiocetidae, *Llanocetus*, *Mystacodon*, *Maiabalaena* and *Coronodon*) and early chaemysticetes (i.e., Eomysticetidae and *Sitsqwayk*) show archaeocete-like morphological patterns of the vertex in that the nasofrontal suture is located at the anterior border of the interorbital region of the frontal (with the exception of *Aetiocetus polydentatus*, in which the nasofrontal suture is located well within the interorbital region of the frontal); the anterior border of the nasal is located at a considerable distance from the frontal, reaching a point located between one-third and half of the length of the maxilla; the ascending process of the maxilla is present, narrow and triangular in outline, forming an evident angle with the posterolateral border of the maxilla; the frontal is flat and wide along both the anteroposterior and the transverse axes; the frontal-parietal (coronal) suture is developed transversely; and the postorbital constriction is transversely narrow and long.

This pattern undergoes numerous changes in the Balaenomorpha in all the structures mentioned above. The nasofrontal suture is retained at the anterior border of the interorbital region of the frontal in the Balaenoidea and basal thalassotherian taxa but it is located more posteriorly within the interorbital region of the frontal in the Cetotheriidae and Balaenopteroidea. The posterior development of the nasofrontal suture is paralleled by an anterior shift of the anterior border of the parietal, which in Balaenopteroidea and some cetotheriid taxa is located more anteriorly than the posterior-most point of the maxilla. This configuration results in an anteriorly concave coronal suture and in a massive reduction in the size of the interorbital region of the frontal, which may be completely superimposed by the posteromedial elements of the rostrum (ascending process of maxilla, ascending process of the premaxilla and nasal). This morphological pattern is traditionally known as ‘telescoping’ [56,63] and was recently reviewed by [64], who analyzed the possible developmental mechanisms underlying suture formation in telescoped cetacean skulls.

In the Balaenoidea and basal thalassotherian taxa, the coronal suture is anteriorly convex. In the Balaenoidea, it is completely superimposed by a massive anterior projection of the supraoccipital that reaches the posterior portion of the interorbital region of the frontal and, consequently, a shortening of the interorbital region of the frontal is due to the anterior thrust of the supraoccipital that excludes the parietal from being observed in dorsal view (Figure 11). Moreover, the ascending process of the maxilla is reduced in length. The balaenoid pattern is also observed in the earliest known balaenoid species, *Morenocetus parvus*, which shows a less advanced degree of bone overlap between the rostrum and frontal so that the interorbital region of the frontal is anteroposteriorly longer in comparative terms than in other, later balaenoid taxa. Despite the longer interorbital region of the frontal, the ascending process of the maxilla is short, as suggested by the extent of the articular groove between maxilla and frontal, even though there would be enough space to allocate a longer ascending process of the maxilla. This pattern is in contrast with the hypothesis that the length of the interorbital region of the frontal is related to the available space in the interorbital region of the frontal suggested by [65] and indicates that different developmental mechanisms may be responsible for the patterning of these two anatomical structures.

In basal thalassotherian taxa, the coronal suture is anteriorly triangular, and the parietal is superimposed on the posterior portion of the interorbital region of the frontal. In this way, the interorbital region is consistently shortened along the anteroposterior axis being constricted between the anterior border of the parietal posteriorly and by the wide, triangular and short ascending processes of the maxilla anteriorly (Figure 12).

In conclusion, in early mysticetes, the vertex closely resembles that of the basilosaurine and dorudontine archaeocetes. The articulation between the rostrum and the frontal is the major difference since in early mysticetes it is realized exclusively by the ascending process of maxilla and premaxilla, and the posterolateral border of the maxilla and the anterior border of the frontal are spaced. At the same time, it was concluded that the evolution of the rostrum, including the vertex structure, underwent a remarkable diversification in the Balaenomorpha with the evolution of two main styles, as follows: (1) anteriorly

convex coronal suture, short and wide ascending process of the maxilla and premaxilla in the Balaenoidea and basal thalassotherian taxa; and (2) anteriorly concave coronal suture, long and narrow ascending process of the maxilla in Cetotheriidae and Balaenopteroidea. Fine differences are then observed within these two main patterns: (i) development of the superimposition of the supraoccipital on the posterior portion of the interorbital region of the frontal in the Balaenoidea but not in basal thalassotherian taxa, and (ii) the ascending processes of the maxilla meet along the longitudinal axis of the skull in the Cetotheriidae but not in the Balaenopteroidea.

### 3.3. Temporal Fossa

In basilosaurine and dorudontine archaeocetes, the temporal fossa has an anteroposteriorly elongate, oval shape (Figure 8). The anterior portion of the temporal crest for the attachment of the temporalis muscle is located at the posterodorsal edge of the flat supraorbital process of the frontal and continues along a sagittal crest located on the top of the skull up to the anterior edge of the supraoccipital. The temporal crest projects posterolaterally to a posterior apex named the nuchal crest. Finally, the temporal crest projects anterolaterally from the nuchal crest along the dorsal edge of the squamosal where it may form a prominent supramastoid crest. In the archaeocetes illustrated in Figure 8, the nuchal crest is triangular and protrudes posteriorly, reaching a point that is located more posteriorly than the occipital condyle. This pattern is retained in some of the earliest-diverging mysticetes, such as *Coronodon*, *Llanocetus* and *Mystacodon*, and in some balaenomorph mysticetes, such as the basal thalassotherians *Pelocetus*, *Atlantocetus* and *Uranocetus* (Figure 12).

The position of the orbitotemporal crest at the posterodorsal edge of the supraorbital process of the frontal is retained in all the toothed mysticetes (Mammalodontidae, Aetiocetidae, *Coronodon*, *Llanocetus* and *Mystacodon*) and eomysticetes. Among the Balaenomorpha, only the Cetotheriidae retains this character. In all the other balaenomorph baleen whales, the orbitotemporal crest shows different shapes. In the Balaenoidea and basal thalassotherian taxa, the orbitotemporal crest is developed from an anteromedial point to a point close to the postorbital process, diagonally crossing the supraorbital process of the frontal (Figure 12E). In the Balaenopteroidea, the orbitotemporal crest forms a wide posterior concavity because most of its development occurs close to the anterior border of the supraorbital process of the frontal.

The temporal crest (which runs parallel to the lateral borders of the supraoccipital) overhangs the temporal fossa and prevents the posterior portion of the parietal and the anterior part of the squamosal from being exposed in dorsal view in the Balaenoidea and late Balaenopteridae. As observed in the advanced archaeocetes, toothed mysticetes, early chaeomysticetes, basal thalassotherian taxa and cetotheriids, the plesiomorphic condition consists of a temporal crest that does not overhang the temporal fossa and the posterior parietal so that the anterior part of the squamosal can be observed in dorsal view. Even the earliest known balaenoid species, *Morenocetus parvus*, shows the plesiomorphic state, in which the temporal crest does not overhang the temporal fossa [66]. In the Balaenopteridae, early-diverging species (e.g., *Archaeobalaenoptera castriarquati*, '*Balaenoptera*' *ryani*) may show the plesiomorphic condition but, in general, the temporal crest does overhang the temporal fossa like in extant and fossil balaenoids (with the exclusion of *M. parvus*).

In the Balaenomorpha, the anteroposterior length of the temporal fossa is visibly diminished, paralleling the shortening of the intertemporal constriction. The geometry of the temporalis muscle and the shape of the *ensemble* formed by the orbitotemporal, temporal, nuchal and supramastoid crests show morphological patterns that are largely different from those observed in nonbalaenomorph mysticetes. Again, the origin of the Balaenomorpha marked the beginning of a diversification process in mysticete morphology.

### 3.4. Occipital Region

In ([64], p. 1062), Roston and Roth define the term telescoping in reference to skulls that have “(i) extensive bone overlap and (ii) extreme proximity of anterior and posterior cranial elements that is observed in modern cetaceans”. In mysticetes, the second feature is attained by a posterior elongation of the posteromedial elements of the rostrum together with an anterior placement of the anterior border of the supraoccipital. In the earliest-diverging mysticetes, such as the Mammalodontidae, *Mystacodon*, *Coronodon*, *Fucaia* and some aetiocetids (including *Aetiocetus cotylalveus*), the anterior apex of the supraoccipital is located on a transverse line crossing the skull posteriorly to the posterior border of the temporal fossa. The advanced aetiocetid *Aetiocetus polydentatus*, however, shows a more anterior placement of the anterior apex of the supraoccipital, which is located anteriorly to the posterior border of the temporal fossa. This pattern is observed in eomysticetids, *Maiabalaena* and *Sitsqwayk* and is retained by balaenomorph mysticetes. In all the nonbalaenomorph mysticetes, the anterior apex of the supraoccipital is located more posteriorly than the anterior end of the zygomatic process of the squamosal. This pattern is not retained in balaenomorph mysticetes, in which the supraoccipital reaches a point that is more anterior than the anterior end of the zygomatic process of the squamosal. The cetotheriids are an exception in that they are the only balaenomorph family in which the anterior apex of the supraoccipital is posterior to the anterior end of the zygomatic process of the squamosal [56,63]. The origin of the Balaenomorpha marks a major shift in supraoccipital development with a supraoccipital that develops more anteriorly, superimposing onto the cranial vault and reducing the anteroposterior extent of the parietal exposure in dorsal view. In the case of the Balaenoidea, the supraoccipital completely excludes the parietal from dorsal exposure. In the Balaenopteroidea, a complex system of sutures occurs at the supraoccipital–parietal interface; the eschrichtiids show the presence of a bony block interposed between the anterior end of the supraoccipital and the interorbital region of the frontal that was interpreted as an interparietal [67], which is not separated from the supraoccipital itself. This structure forms a platform anterior to the anterior border of the supraoccipital and replaces the sagittal crest observed in the archaeocetes, early-diverging mysticetes and basal thalassotherian taxa with a couple of externally concave attachment sites for the temporalis muscle connected to the orbitotemporal crest anteriorly and to the temporal crest posteriorly. This same morphological pattern is observed in the Cetotheriidae. In the Balaenopteridae, the intertemporal constriction is transversely wider, and the interparietal, when present, is anteroposteriorly reduced to a thin sheet of bone interposed between the anterior border of the supraoccipital and the interorbital region of the frontal (see [62] for an overview).

The anterior border of the supraoccipital is wide and round in archaeocetes, and the supraoccipital is mainly developed along the dorsoventral axis. A rounded outline is also observed in the Mammalodontidae (Figure 8), *Fucaia* and *Aetiocetus cotylalveus*, but a triangular outline is present in *Llanocetus*, *Mystacodon*, *Coronodon* and *Aetiocetus polydentatus* (Figure 9). The triangular shape is shared with later chaemysticetes, including the Eomysticetidae, basal thalassotherian taxa, early balaenopterids and some cetotheriids. The triangular shape of the supraoccipital is thus an evolutionary novelty that originated in the period between the origin of the Mysticeti and the origin of the Balaenomorpha.

Another evolutionary novelty that appeared independently in different balaenomorph clades is the transverse expansion of the intertemporal constriction, which can be related to the increase in the transverse width of the anterior border of the supraoccipital in the advanced balaenopterids and in *Eubalaena*. This character was discussed in [50] in relation to the anterior expansion of the forebrain of the extant Balaenopteridae. Such an expansion is observed in later balaenopterids (genera *Balaenoptera*, *Megaptera*, *Norrisanima* and *Diunatans*) and in the Balaenoidea. Additional work is necessary to properly define this expansion in order to improve our understanding of its relation-

ships with the enlargement of the anterior portion of the frontoparietal lobes of the rostral brain.

Several accounts illustrated the posterior view of archaeocete (e.g., [27,68]) and mysticete (e.g., [11,19,29,30,33,43,69,70]) skulls. Based on these accounts, it is possible to observe that the exoccipital protrudes laterally and forms an approximately right angle with the supraoccipital in archaeocetes. In the mysticetes, the exoccipital protrusion is less marked as the posterior width of the supraoccipital is wider compared to that of archaeocetes, and the angle is obtuse. In many cases (e.g., balaenids) the angle cannot be observed because the lateral border of the supraoccipital and the borders of the exoccipital are continuous.

In more general terms, in dorsal view, the archaeocete occipital region shows a transverse constriction at the level of the nuchal crest (Figure 8A–C); this constriction was already lost in the earliest-diverging mysticetes (Mammalodontidae) because of the larger distance between the posterior apices of the nuchal crest (Figure 8D,E).

Finally, a change in supraoccipital orientation occurred at the Mysticeti node: in the archaeocetes, the supraoccipital is mostly developed along the dorsoventral axis, but in the mysticetes it projects anteriorly and superimposes on the parietal. The anterior shift of the supraoccipital is one of the key points related to the concept of telescoping in the cetacean skull [56,63,64].

### 3.5. Earbones

Extensive descriptions and comparisons of the mysticete earbones have been published in the last decade, including, for example, those of [26,71–73]. Periotic and cochlear morphologies have been intensely studied by CT scans and 3D renderings showing resemblances between the mysticetes and later archaeocetes [73]. Tomographic analyses of the mammalodontid and aetiocetid cochleae revealed that the earliest-diverging mysticetes had cochlear morphologies similar to those of the archaeocetes rather than those of the chaemysticetes [72]. This observation suggests that both the advanced archaeocetes and the earliest-diverging mysticetes could share the characteristic of low-frequency hearing with the Chaemysticeti [72].

This suggestion is reinforced by bullar morphology. In Figure 15, schematic representations of the tympanic bullae of the archaeocetes and mysticetes are plotted around the mysticete phylogeny adopted in the present paper. As shown, the archaeocetes and early-diverging mysticetes share the absence of the anterior lobe and the presence of an extended median furrow. In general, the bulla of archaic, nonbalaenomorph mysticetes is morphologically similar to that of the basilosaurine and dorudontine archaeocetes [41]. In a group of basal thalassotherian taxa (including the genera *Diorocetus* and *Parietobalaena*) and in the cetotheriids, the tympanic bulla retains the lack of the anterior lobe; the anterior lobe occurs in a diverse group of basal thalassotherian taxa (including the genera *Atlantocetus* and *Uranocetus*), in the Balaenoidea and in the Balaenopteroidea. Observing the distribution of this character in the phylogeny of Figure 15, it appears that the anterior lobe evolved independently in these three lineages. Further work is necessary to understand the function of the anterior lobe of the tympanic bulla because it is still unclear what function this structure may have in the hearing physiology of the mysticetes.

In conclusion, the earliest mysticetes share a number of characters of both the tympanic bulla and the cochlea, with the later archaeocetes suggesting that they shared similar hearing characteristics. Evident structural changes occurred in the tympanic bulla after the divergence of the main balaenomorph clades with the recurrent evolution of the anterior lobe in the tympanic bulla.

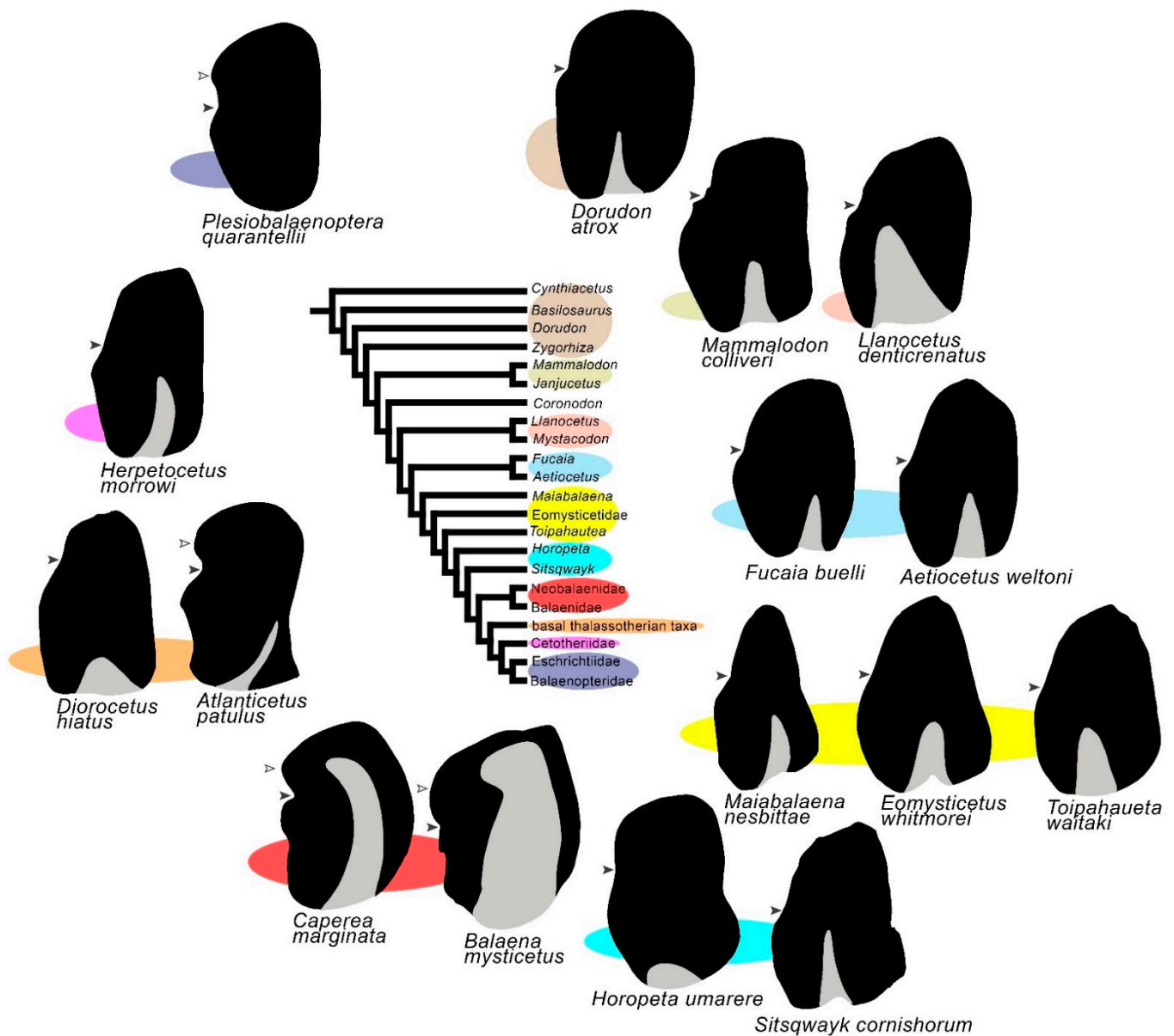


**Figure 15.** Schematic representations of tympanic bullae of advanced archaeocetes and mysticetes in relation to mysticete phylogeny. The black arrowhead indicates the position of the lateral furrow; the gray triangle indicates the position and extent of the median furrow; the white arrowhead indicates the anterior lobe in Balaenopteridae, Balaenoidea and in a group of basal thalassotherian taxa (here represented by *Atlantocetus patulus*). Note the similar extent of the median furrow and the anterior widening of the tympanic bulla in neobalaenids and balaenids. Color ellipses link bullae to the corresponding taxa in the cladogram.

### 3.6. Dentary

Mysticete dentaries were the subject of several studies in recent times in the framework of broader biomechanical and allometric research projects resulting in a wealth of published works (e.g., [17,25,74–79]). Mandibular morphology is linked to feeding styles in extant mysticetes [5,36] and, reasonably, also in early-diverging mysticetes and archaeocetes.

In Figure 16, the dentaries of archaeocetes and nonbalaenomorph mysticetes are represented in lateral view. It is evident that the mammalodontid dentary closely resembles that of the archaeocetes in retaining functional dentition and in having a high and wide coronoid process, posteriorly protruded mandibular condyle and short mandibular ramus.

In this sense, there is evolutionary continuity in the mandibular morphology across the transition from archaeocetes to mysticetes. Morphological and dimensional changes are observed in the subsequent clades. The mandibular ramus of *Mystacodon*, *Fucaia* and *Aetiocetus* is comparatively longer so the distance between condyle and coronoid process is proportionally shorter than that observed in the archaeocetes and *Mammalodon*. Even though the coronoid process is high, in the Aetiocetidae it is comparatively reduced in height with respect to the Mammalodontidae and archaeocetes.

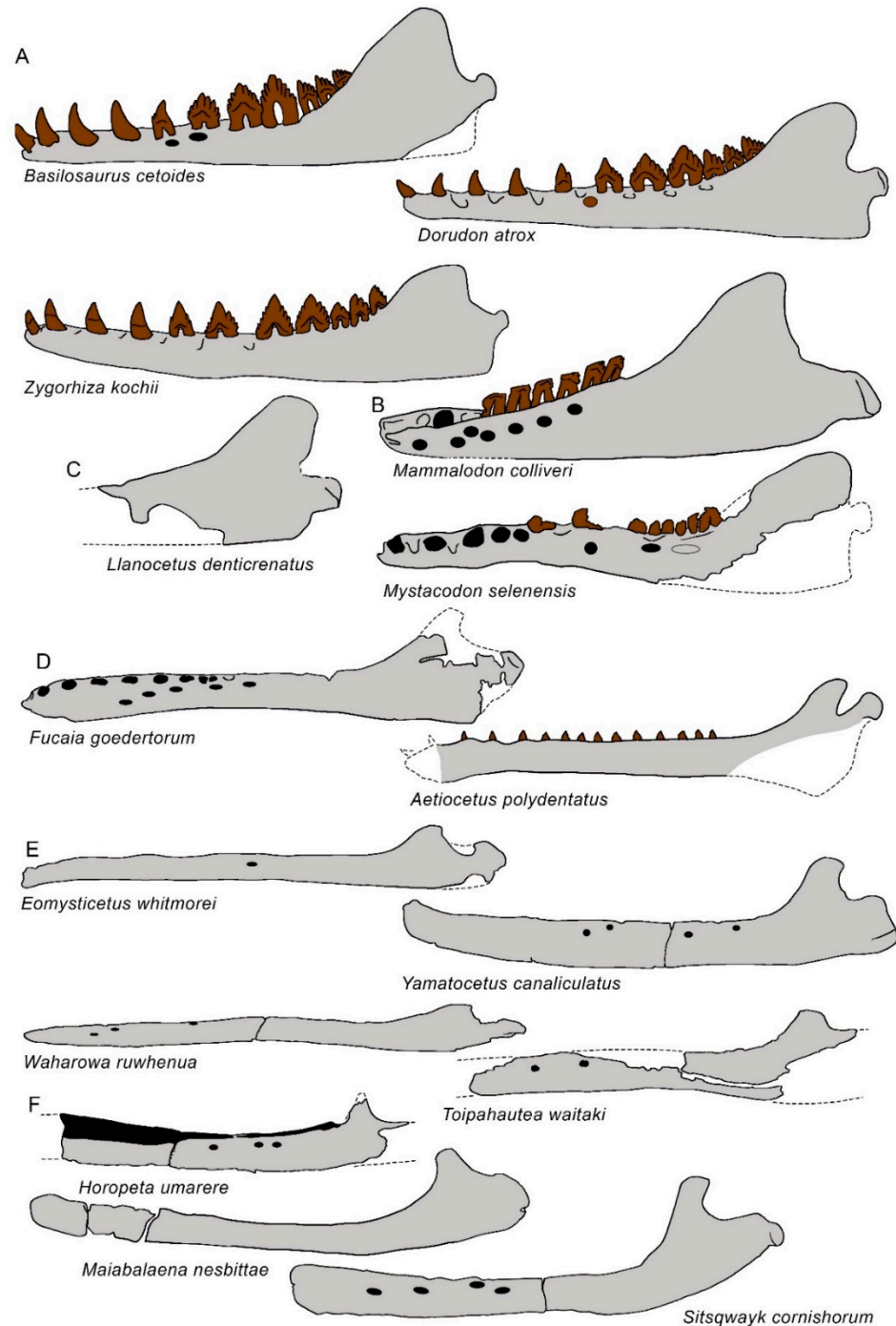


**Figure 16.** Schematic representations of the dentary of advanced archaeocetes and nonbalaenomorph mysticetes in lateral view. (A) Archaeocetes. (B) Mammalodontidae. (C) Other early diverging mysticetes. (D) Aetiocetidae. (E) Eomysticetidae. (F) Stem-Balaenomorpha and *Maiabalaena nesbittae*. Not to scale. Dentaries are represented as if they shared the same anteroposterior length.

The dentary of the later-diverging, nonbalaenomorph mysticetes shows massive elongation of the mandibular ramus and reduction in the height of the coronoid process together with definitive tooth loss. This pattern is emphasized in the dentaries of the Balaenomorpha (Figure 17), in which the coronoid process is low and the mandibular ramus is edentulous and massively elongated. The coronoid process may become difficult to observe due to its extreme reduction in some taxa, such as the Balaenoidea, Eschrichtiidae and the cetotheriid *Cetotherium riabinini* [80]. As shown in [67], a character related to the origin of the Chaemysticeti is the external torsion of the coronoid process. This character is observed in *Toipahautea* and in all the other chaemysticete cetaceans but not in the Aetiocetidae, Mammalodontidae and the other earliest-diverging mysticetes.

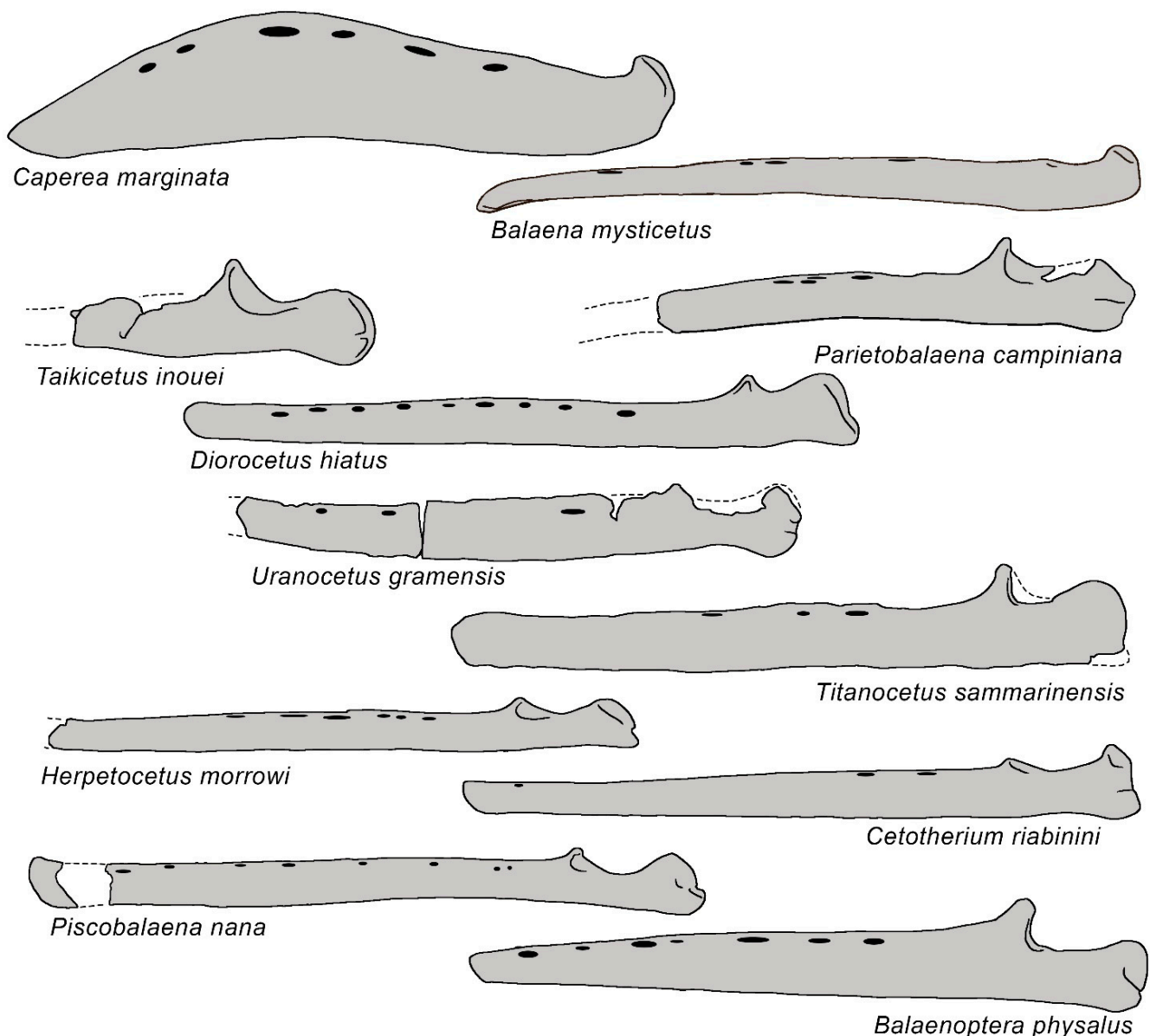


**Figure 17.** Schematic representations of the dentary in Balaenomorpha in lateral view. Not to scale. Dentaries are represented as if they shared the same anteroposterior length.

In medial view, several morphological transformations occurred during the evolution of the earliest mysticetes. In Figure 18, the medial views of the dentaries of the nonbalaenomorph mysticetes are shown. Interestingly, neither *Mammalodon* nor *Coronodon* show the symphyseal morphology of the later-diverging mysticetes, in which a groove for the mental ligament is developed at the anterior end of the mandibular ramus. A groove is

observed in the Aetiocetidae and in the subsequent mysticete radiations, suggesting that this character was not part of the morphological *suite* typical of the earliest mysticetes. The mandibular foramen is invariably wide, resembling that of the extant odontocetes and thereby suggesting a similar function (as suggested also by [81]). As shown in Figure 19, the mandibular foramen is also large in several balaenomorph clades, including basal thalassotherian taxa and cetotheriids (see also [36]). It is largely reduced in the Balaenoidea and Balaenopteridae.

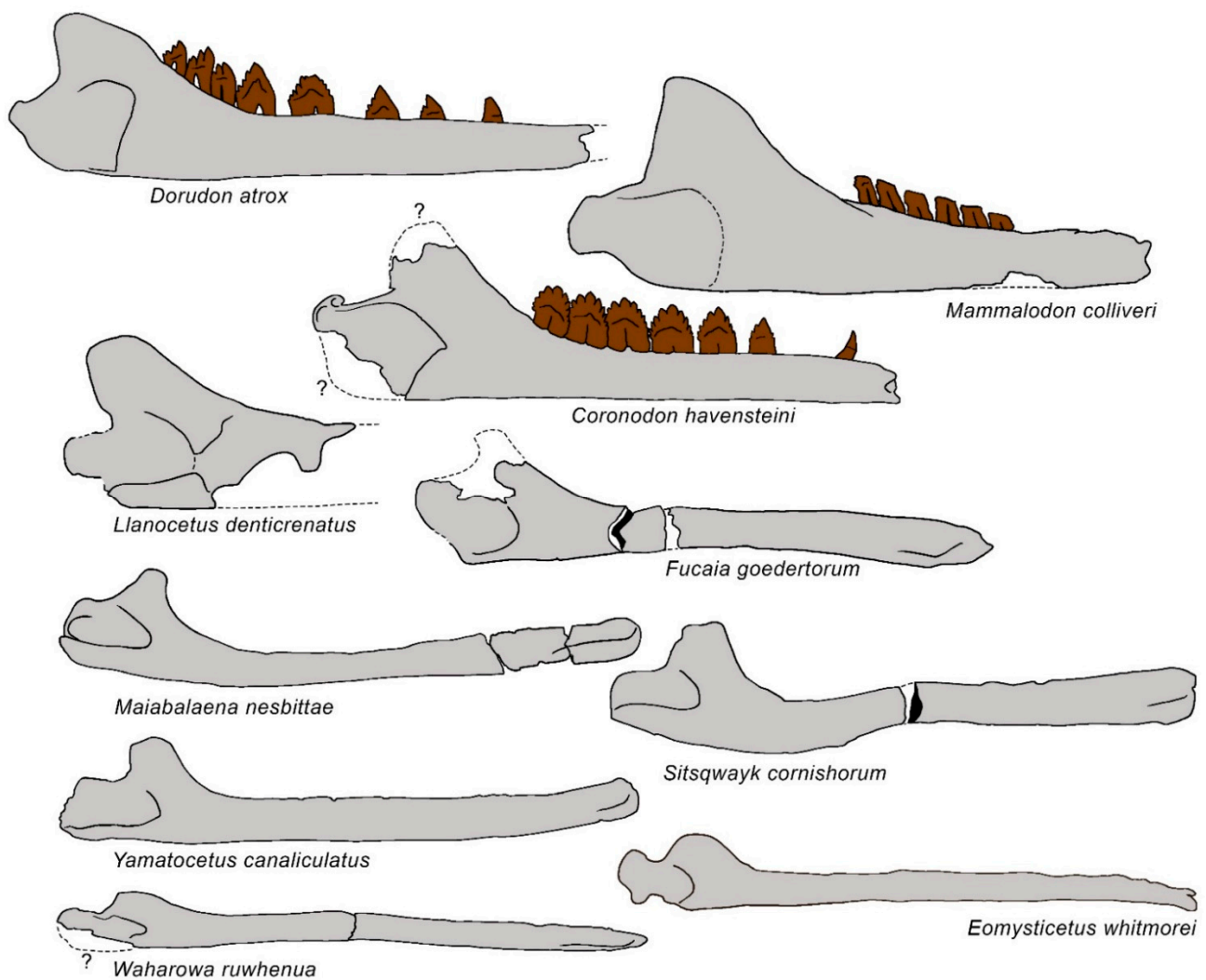


**Figure 18.** Schematic representations of the dentary of advanced archaeocetes and nonbalaenomorph mysticetes in medial view. Not to scale. Dentaries are represented as if they shared the same anteroposterior length.

The external curvature of the mysticete dentary was analyzed in [76,82]; in these studies, a relation was discovered between the curvature itself and the way in which the dentary is depressed during the opening of the mouth. In particular, in extant balaenopterids, the dentary rotates externally during the opening of the mouth, allowing baleen to be exposed. The earliest-diverging mysticetes had straight dentaries, and it is reasonable to hypothesize that their dentaries did not rotate externally during the process of the opening of the mouth. A number of balaenomorph mysticetes had straight dentary. These include some balaenopterids (*Protororqualus cuvierii*, *Archaeobalaenoptera castriarquati*) and a single balaenid (*Balaenula astensis*) [51,58,78,83]. It is still unclear which functional consequences had this condition in these balaenomorph mysticetes.

In conclusion, the origin of mysticetes was not marked by morphological changes in the dentary. The morphological transformations occurred more crownward and were characterized by a marked elongation of the mandibular ramus and by the origin of a symphyseal groove certainly from the Aetiocetidae, reduction in and loss of dentition and lowering of the coronoid process in some eomysticetids. The whole *suite* of morphological characters typical of the dentary of extant mysticetes was present at the Balaenomorpha node (elongated ramus, reduced and deflected coronoid process, dentition absent, external curvature of the dentary in dorsal view). The reduction in the mandibular foramen occurred independently in the Balaenoidea and Balaenopteroidea while a wide mandibular foramen is present in the basal thalassotherian taxa and Cetotheriidae.

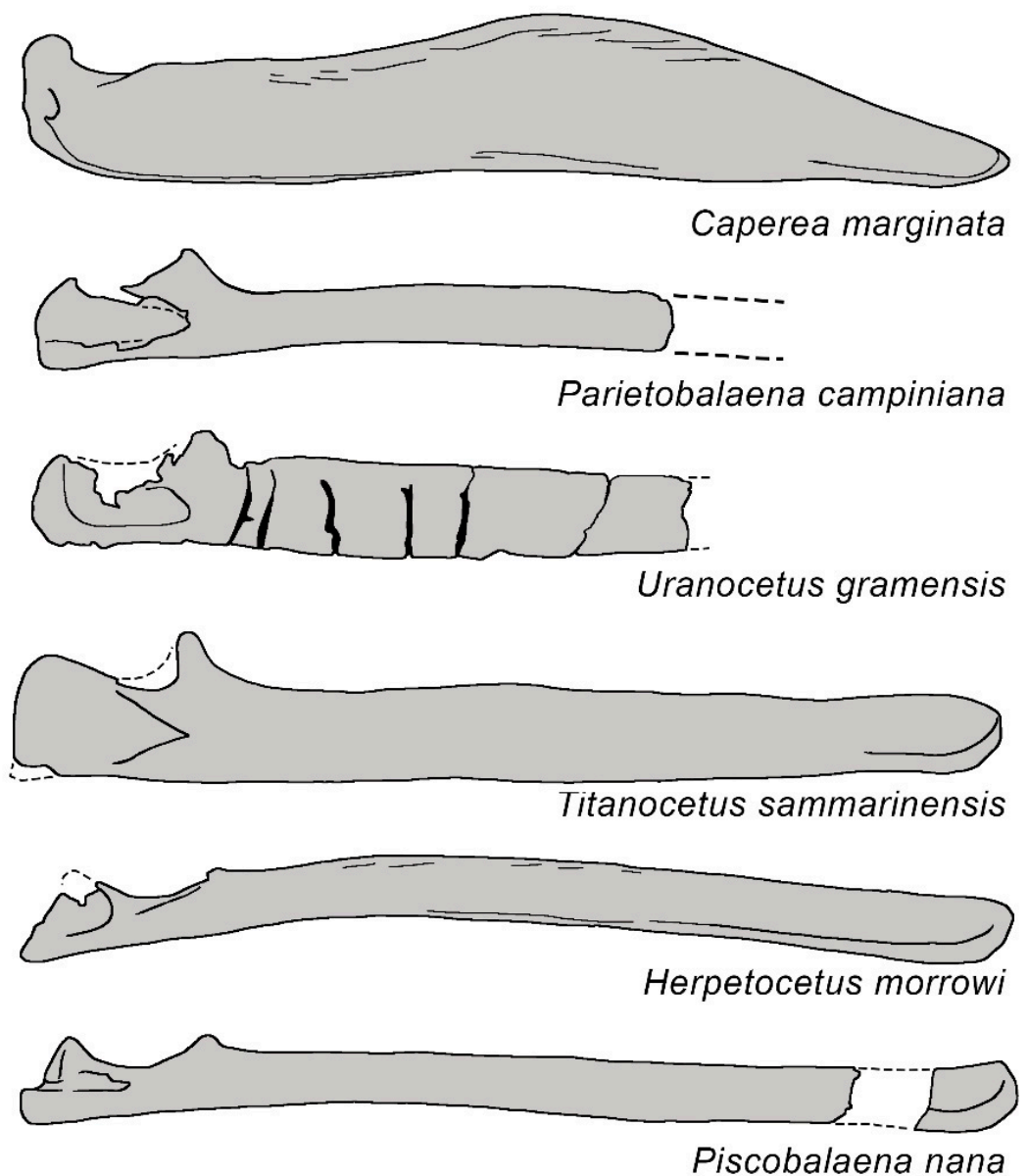


**Figure 19.** Schematic representations of the dentary in Balaenomorpha in medial view. Not to scale. Dentaries are represented as if they shared the same anteroposterior length.

### 3.7. Appendicular Skeleton

The evolution of the vertebral column of baleen whales is scarcely known. Usually, new mysticete taxa are diagnosed based on skull and earbone characters and limited space is devoted to the description of vertebral and appendicular skeleton. This is a major limit to the development of better knowledge of the evolution of the postcranial skeleton of mysticetes. A few works have been dedicated to the functional morphometry of mysticete skeletons (e.g., [84–87]), but a systematic analysis of the different morphological and morphometric patterns exhibited by the member of this group remains elusive. For this reason, we abstain from trying to infer evolutionary patterns based on the morphometric characters of the vertebral column and focus on the appendicular skeleton that has been described and studied for many fossil and extant taxa.

In Figure 20, the scapulae of four archaeocetes and four early-diverging mysticetes are shown. The scapula of *Mystacodon selenensis* (a nonchaemysticetid mysticete) is almost indistinguishable from that of the archaeocetes due to having the following morphological characters: (1) a posteroventrally concave margo caudalis, (2) a wide supraspinous fossa and (3) an anteroventrally convex margo cranialis. In Figure 21, the scapulae of selected balaenomorph mysticetes are shown. In all the balaenomorph mysticetes, the supraspinous fossa is visibly reduced as the scapular spine projects more anteriorly than in nonbalaenomorph mysticetes. Moreover, in all the balaenomorph mysticetes (with the exception of Balaenidae), the scapula appears to be more elongated along the anteroposterior axis because the margo caudalis projects posteriorly in a sharper way than in nonbalaenomorph mysticetes. A similar pattern is observed in the margo caudalis of *Sitsqwayk* but not in *Horopeta*, whereas the supraspinous fossa of *Horopeta* is less extended than that of *Sitsqwayk*. These observations suggest that the assembly of the typical balaenomorph scapula occurred through a complex evolutionary path and some characters likely originated independently in different lineages (e.g., reduction in the supraspinous fossa and elongation of the margo caudalis). The supraspinous fossa is the attachment site of the supraspinous muscle that is attached, at its distal extremity and through a tendon, to the greater tuberosity of the humerus. Its function consists in the abduction of the humerus. The reduction in the supraspinous fossa observed in balaenomorph mysticetes may be related to a corresponding reduction in the supraspinous muscle and to a decreased ability of humeral abduction in this clade. In turn, this suggests a decreased ability to move the forelimb in the Balaenomorpha, whereas in nonbalaenomorph mysticetes with wide supraspinous fossa, the forelimb abduction should have been similar to that of advanced archaeocetes.

Similarly, the presence of a well-developed deltopectoral crest in archaeocetes and nonbalaenomorph, early-diverging mysticetes suggests that the muscles acting on the medial surface of the humerus were fully functioning, enabling these whales to rotate and abduct the arm in more complex ways compared to balaenomorph mysticetes (Figure 22). A long and protruding deltopectoral crest is retained in *Maiabalaena nesbittae* and in the Eomysticetidae, but that crest is reduced in the stem-balaenomorph *Sitsqwayk cornishorum*. In the latter, the greater tubercle of the humerus is well-developed and protruding, providing additional support for the hypothesis that the supraspinous muscle was well-developed in this species. The reduction in the deltopectoral crest is suggestive of functional loss of motional abilities of the humerus in *Sitsqwayk*, and this is in good agreement with its phylogenetic placement as a stem-balaenomorph taxon. In all the balaenomorph taxa, the deltopectoral crest is so strongly reduced that it cannot be easily individuated in the humeral shaft (Figure 23).

Apart from the process of reduction in the deltopectoral crest, the humerus of all the mysticetes differs from that of the archaeocetes because it lacks the rotational articulation between the humerus, radius and ulna. Rather, two facets are present for distinct articulations, the radial facet and the ulnar facet, which are separated by a transverse crest. This character is a synapomorphy of Neoceti and was present in the common ancestor of Odontoceti and Mysticeti (e.g., [12]).

The principal difference between the radius of the advanced archaeocetes and that of mysticetes is related to the occurrence of a well-developed radial crest at approximately the middle of the height of the anterior border of the radius in the archaeocetes (Figure 24). This crest is absent in the radius of the Eomysticetidae, *Horopeta umarere*, *Sitsqwayk cornishorum* and other chaeomysticetes. This crest represents the attachment site for the quadratus pronatus muscle that acts to pronate the hand. The reduction in or lack of this crest suggests the loss of this function in the mysticetes in which the radial crest is absent.

In the Balaenomorpha, a process of anteroposterior elongation of the distal end of the radius is observed in the Balaenidae, Eschrichtiidae and *Megaptera novaeangliae*. Moreover, the radius is generally more robust in the Balaenomorpha than in nonbalaenomorph mysticetes (Figure 24).

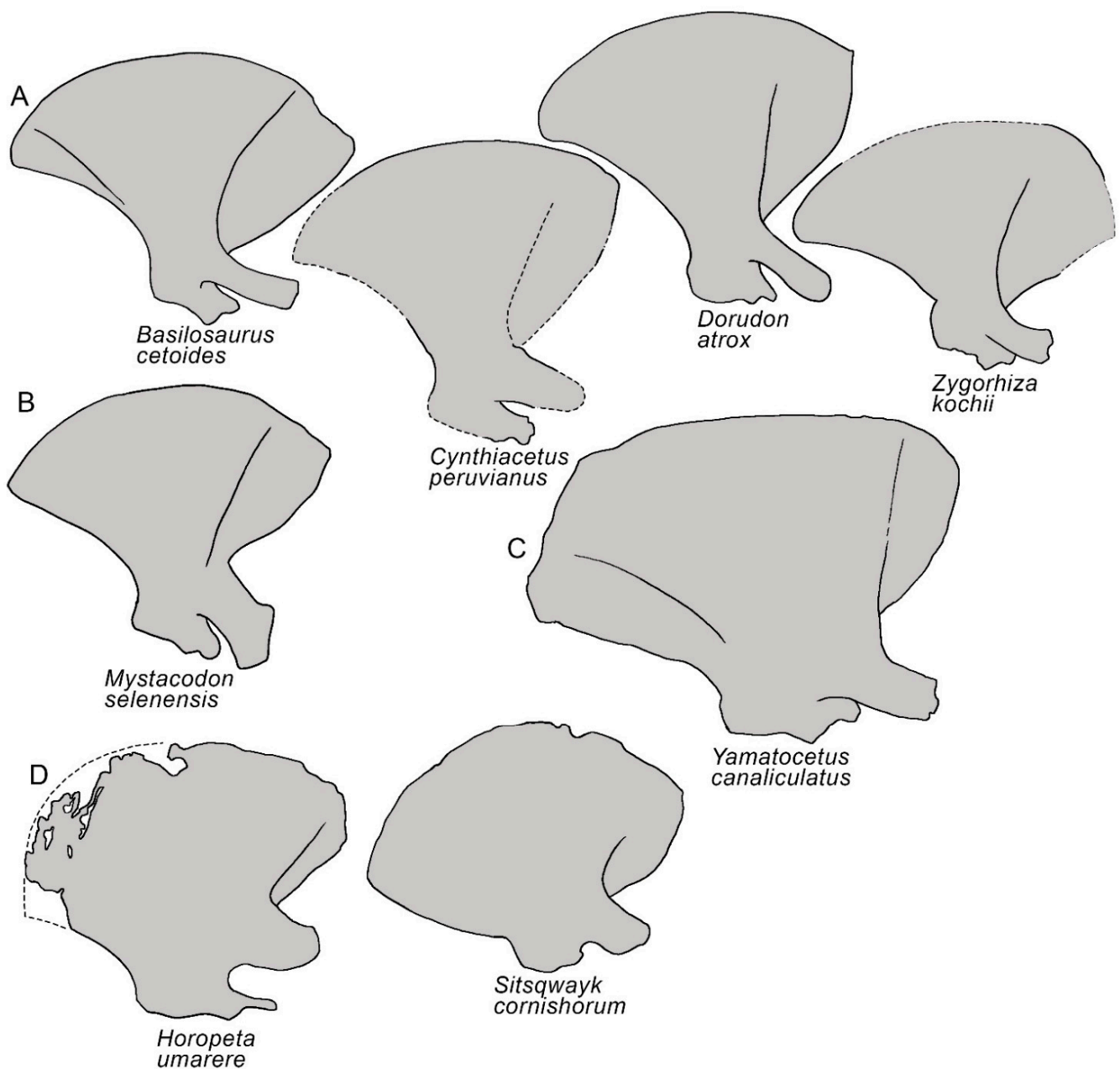


**Figure 20.** Scapulae of archaeocete and nonbalaenomorph mysticetes. (A) Archaeocetes. (B) *Mystacodon selenensis*. (C) The eomysticetid *Eomysticetus whitmorei*. (D) Stem-Balaenomorpha. Not to scale. The scapulae are represented as if they shared the same anteroposterior length.

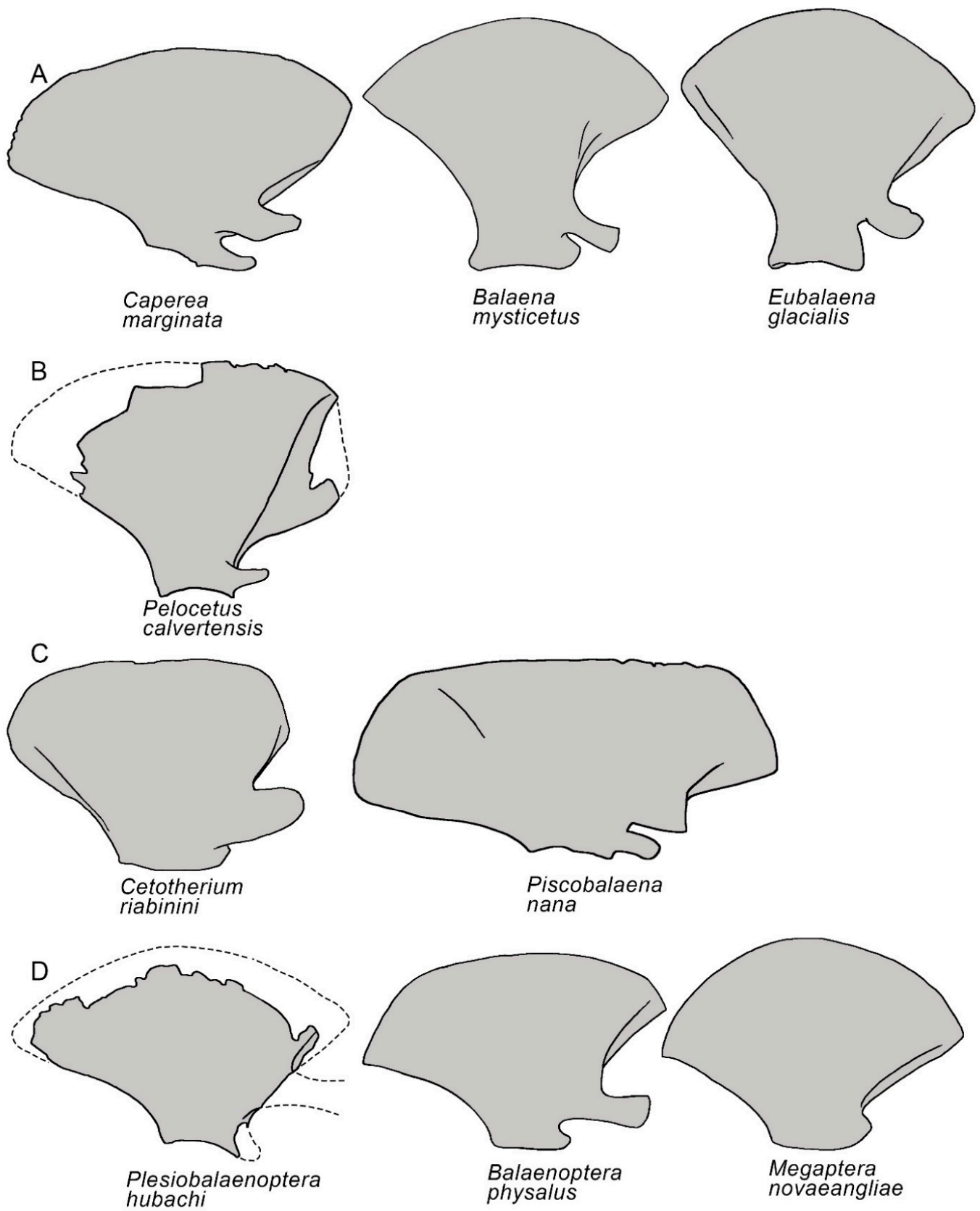


**Figure 21.** Scapulae of balaenomorph mysticetes. (A) Balaenoidea. (B) A basal thalassotherian taxon. (C) Cetotheriidae. (D) Balaenopteroidea. Not to scale. The scapulae are represented as if they shared the same anteroposterior length.

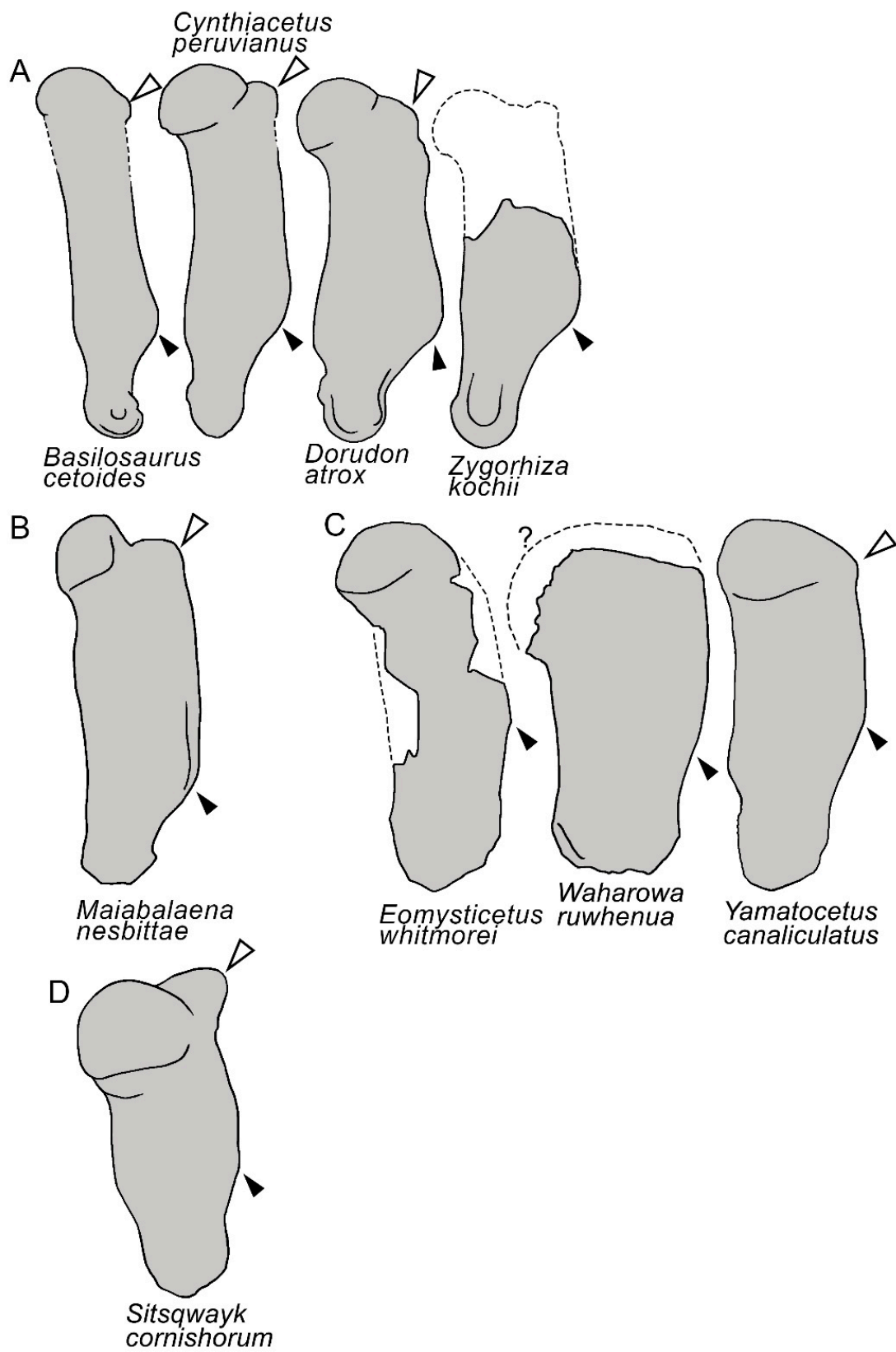


**Figure 22.** Humerus of archaeocetes and nonbalaenomorph mysticetes. (A) Archaeocetes. (B) *Maiabalaena nesbittae*. (C) Eomysticetidae. (D) *Sitsqwayk cornishorum*. The white triangle indicates the greater tubercles of the humerus. The black triangle indicates the maximum extension of the deltopectoral crest. Not to scale. The scapulae are represented as if they shared the same anteroposterior length.

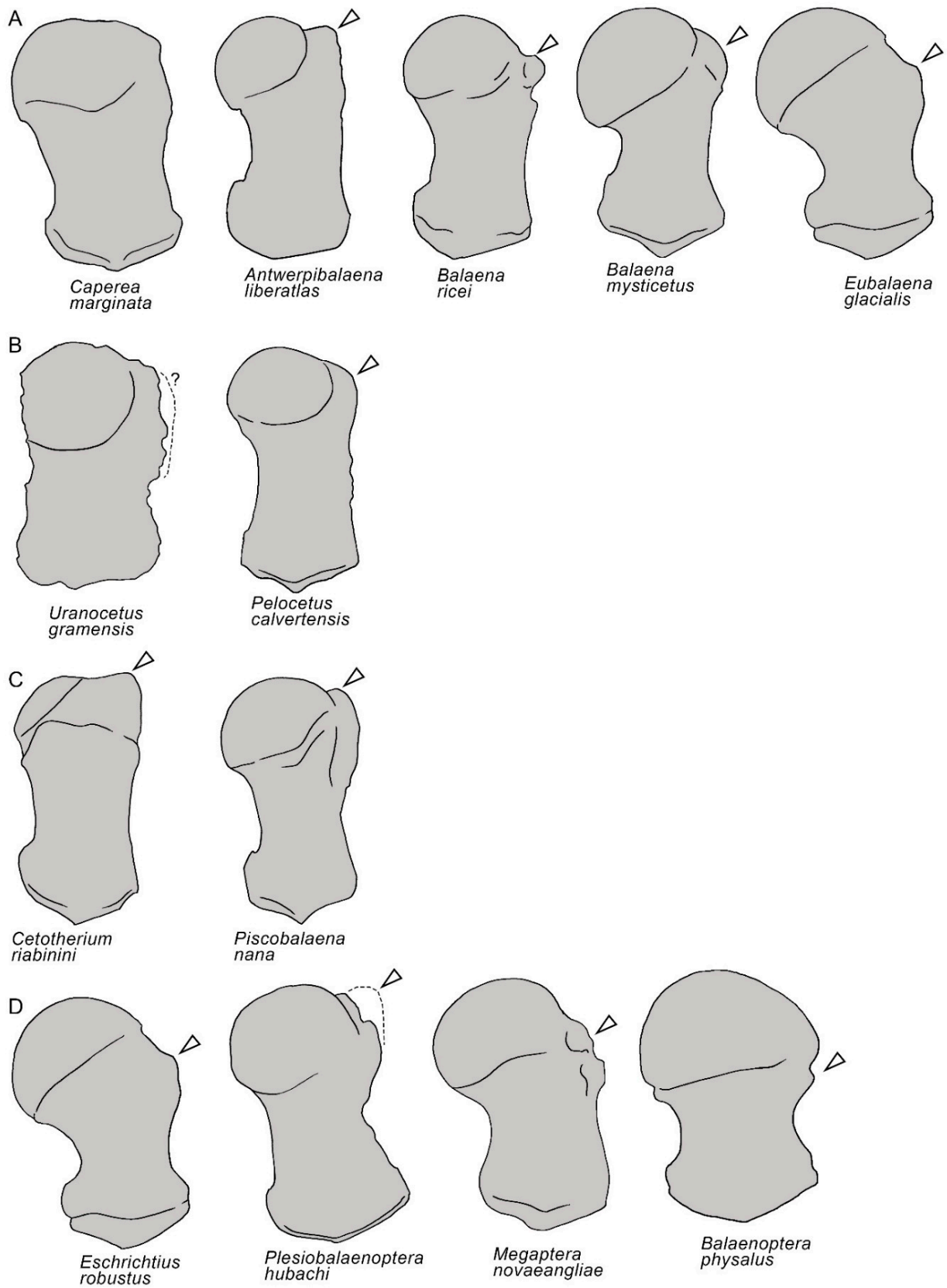


**Figure 23.** The humerus of balaenomorph mysticetes. (A) Balaenoidea. (B) Basal thalassotherian taxa. (C) Cetotheriidae. (D) Balaenopteroidea. The white triangle indicates the greater tubercle of the humerus. Not to scale. The scapulae are represented as if they shared the same anteroposterior length.

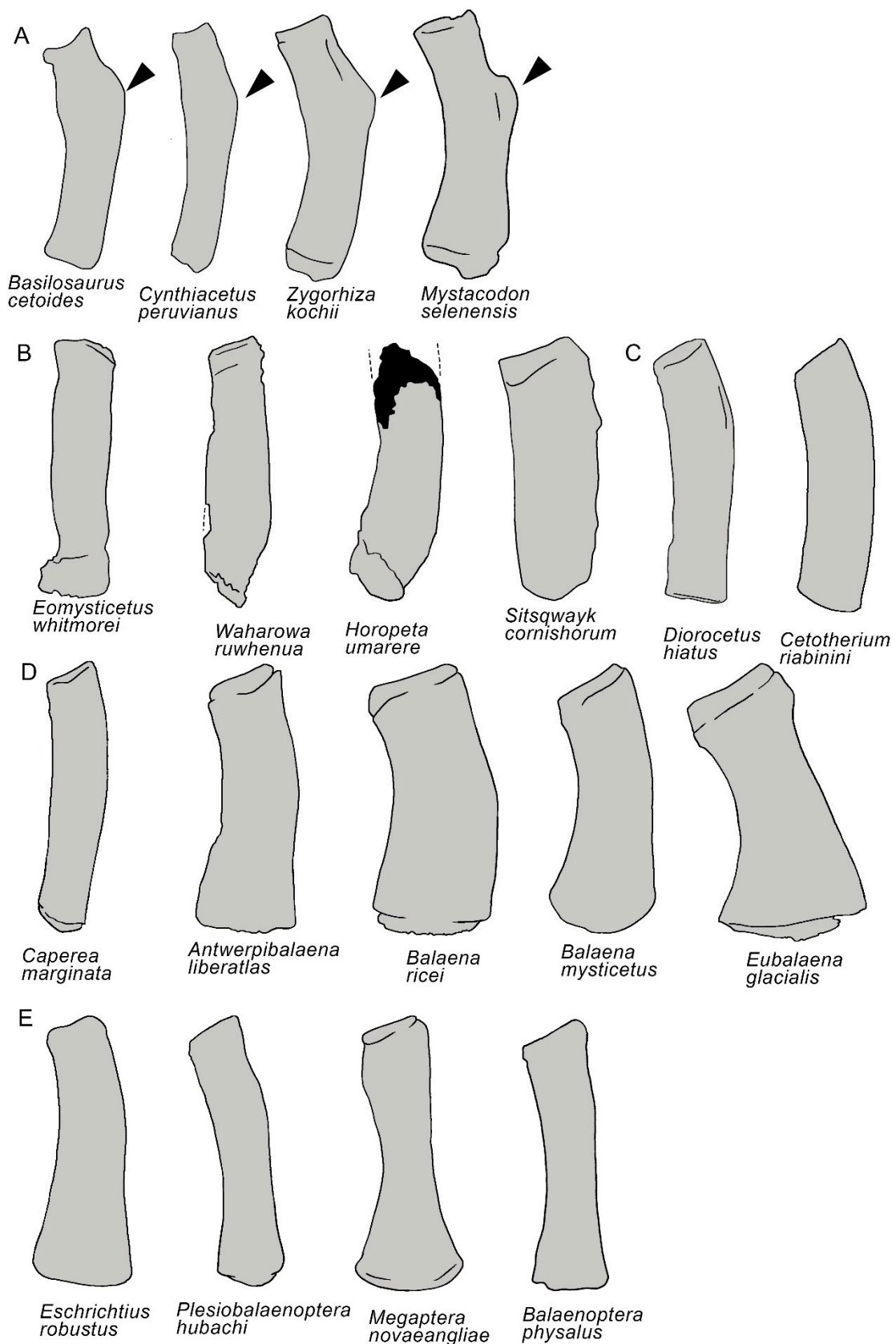


**Figure 24.** Diversity of the radius in mysticete and archaeocete cetaceans. The white triangle indicates the radial crest. (A) Archaeocetes. (B) Eomysticetidae and stem-balaenomorph taxa. (C) A basal thalassotherian taxon and a Cetotheriidae. (D) Balaenoidea. (E) Balaenopteroidea. Not to scale. The scapulae are represented as if they shared the same anteroposterior length.

The ulna of the advanced archaeocetes exhibits a shaft with parallel anterior and posterior borders and an olecranon process whose distal border forms a wide curve with the posterior border of the shaft. In the Eomysticetidae, the morphology of the ulna is variable, with the distal border of the olecranon of *Waharowa ruwhenua* showing the same morphology of the advanced archaeocetes, whereas in *Eomysticetus whitmorei* and *Yamatocetus canaliculatus*, an acute angle separates the distal border of the olecranon from the posterior border of the shaft (Figure 25: white triangle). An acute angle is also present in most Balaenomorpha with the exception of the Balaenidae, in which the angle is lost, and the size and shape of the olecranon process are highly diverse in different species. In particular, in the extant *Eubalaena* species, the olecranon process is highly destructured and reduced to a simple, round protrusion. In the Balaenidae, the distal border of the ulna is expanded at various degrees in different species. In particular, in *Antwerpibalaena liberatlas*, the posterior border of the distal end of the ulna is posteriorly protruded (Figure 25; see also images in [88]); this pattern is similar to that observed in the extant bowhead whale, *Balaena mysticetus*, in which the facet for the articulation with the humerus is flattened and largely destructured. In *Eubalaena glacialis* and *E. australis* (not included in Figure 25), the anterior border of the shaft of the ulna is anteriorly protruded, expanding the surface of the distal epiphysis of the ulna in a remarkable way (Figure 25).

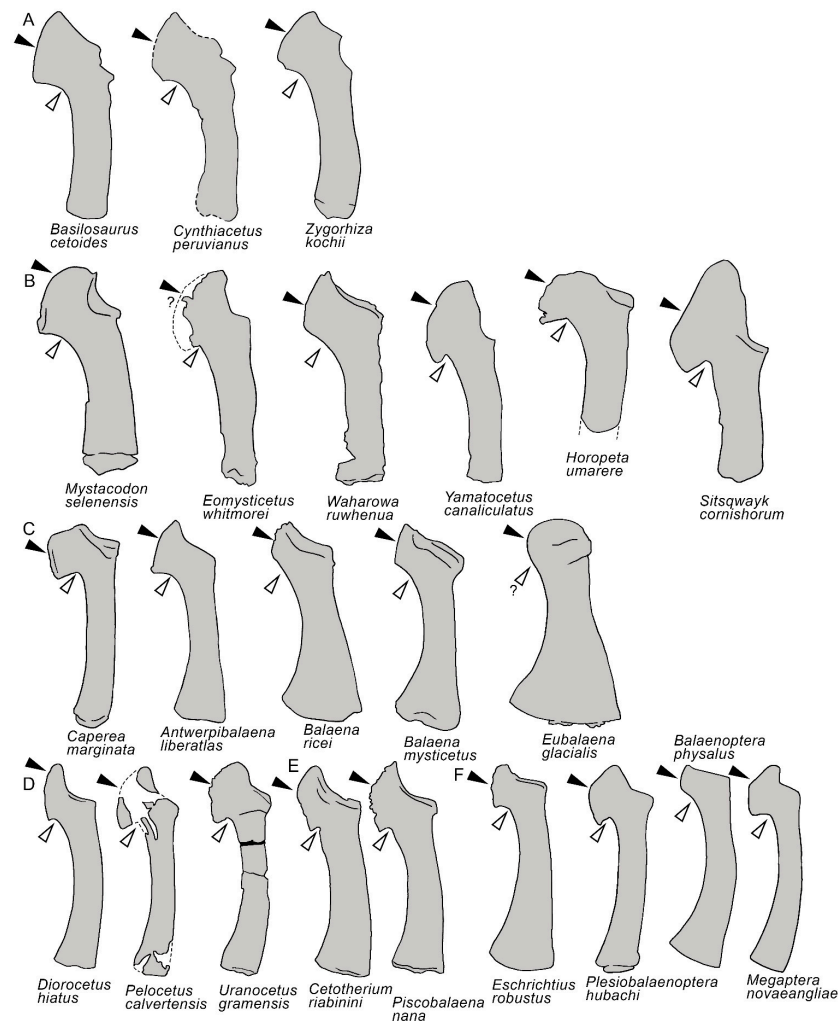


**Figure 25.** Diversity of the ulna in mysticete and archaeocete cetaceans. The black triangle indicates the olecranon process. The white triangle indicates the shape of the distal border of the olecranon process (continuous curve vs. acute angle). (A) Archeocetes. (B) Early-diverging, nonbalaenomorpha taxa. (C) Balaenoidea. (D) Thalassotherii. Not to scale. The scapulae are represented as if they shared the same anteroposterior length.

In conclusion, the origin of mysticetes was marked by two morphological changes of the forelimb. The earliest-diverging mysticetes had a scapula and humerus with the same morphological characters present in advanced archaeocetes, with the exception of the articulation between humerus, radius and ulna, which was not rotational. Moreover, the reduction in and loss of the radial crest suggests that hand movements were already unavailable to the earliest, nonbalaenomorph taxa. These two morphological changes suggest early functional changes in the swimming style of basal mysticetes. However, the precise functional effects provided by these changes are not fully understood.

### 3.8. Reconstruction of Character States at Ancestral Nodes

The distributions of the morphological characters described and discussed above were mapped in the phylogeny of Figure 5, and the character states at ancestral nodes were inferred through the maximum likelihood algorithm as implemented in MESQUITE 3.6 (see Methods). In Figures 26 and 27, the results of the mapping procedure are shown. Only characters 1, 2, 3, 4, 14, 17 and 18 are inferred to be present in the common ancestor of all the mysticetes. These characters show that in the early phases of mysticete evolution, the rostrum was characterized by a considerable number of morphological transformations (character 1: origin of lateral process of maxilla; character 2: origin of the infraorbital plate; and character 3: origin of multiple dorsal infraorbital foramina). The posterior region of the skull underwent morphological transformations with the posterior portion of the lateral border of the supraoccipital that moved laterally, and the transverse constriction in the posterior portion of the supraoccipital was lost (characters 17 and 18). We speculate that the posterior enlargement of the supraoccipital could be related to an expansion of the attachment sites for the neck muscles.

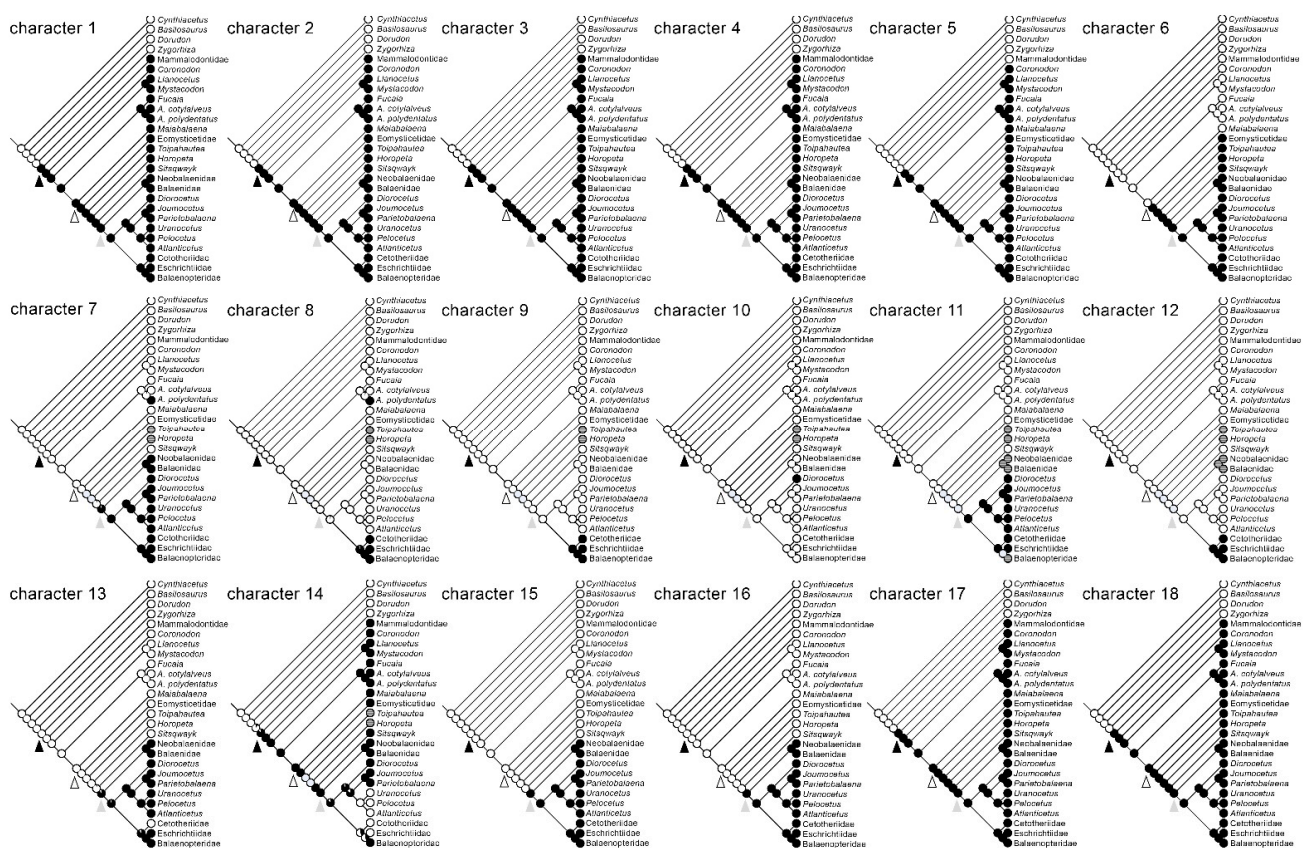


**Figure 26.** Analysis of the distribution of characters 1–18 of Table 2 in the phylogeny of Figure 1. The black triangle corresponds to the Mysticeti node, the white triangle corresponds to Chaemysticeti and the gray triangle corresponds to Balaenomorpha.

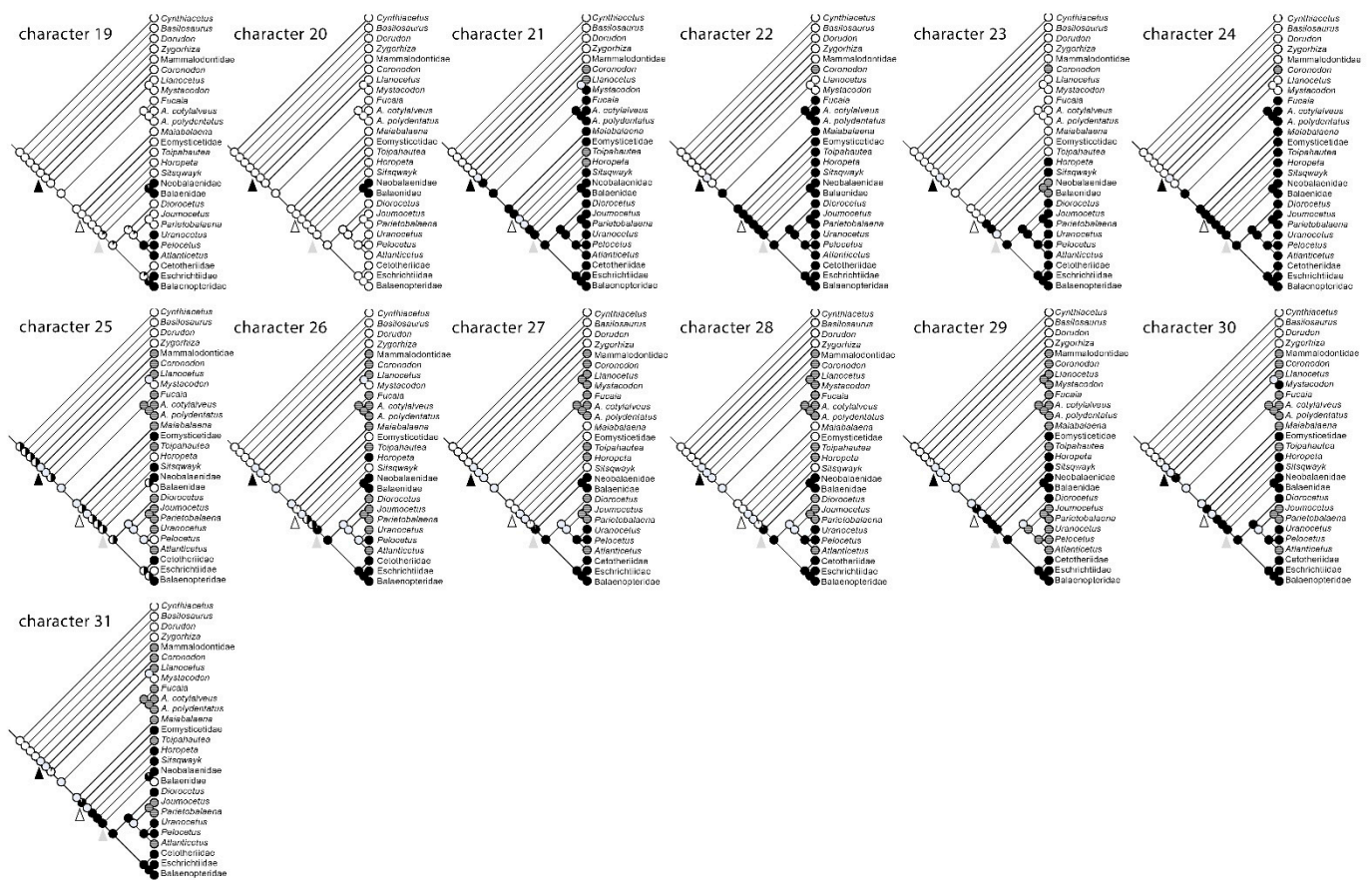


**Figure 27.** Analysis of the distributions of characters 19–31 of Table 2 in the phylogeny of Figure 1. The black triangle corresponds to the Mysticeti node, the white triangle corresponds to Chaecomysticeti and the gray triangle corresponds to Balaenomorpha.

We noticed a large amount of morphological conservatism in the earliest phase of mysticete evolution. For example, the morphology of the tympanic bulla, position of the orbitotemporal crest, shape of the temporal fossa in dorsal view, relative proportions of the mandibular ramus and coronoid process of the dentary retained the same character states of the advanced archaeocetes (characters 13, 15–16 and 21–24). Unfortunately, the postcranial skeleton of the earliest mysticetes is scarcely known, and this prevents a full assessment of the morphological transformations that occurred in the earliest phases of mysticete postcranial evolution. However, based on what is known to date, we observed that all the postcranial characters discussed in the present paper show plesiomorphic (i.e., shared with advanced archaeocetes) states and that the morphological change occurred in the postcranial skeleton of later-diverging mysticetes (see distributions of characters 25–31 in Figure 27).

Three postcranial characters (29, 30 and 31) are inferred to have been originated at the Chaecomysticeti node, including the loss of the radial crest, loss of the rotational articulation between humerus, radius and ulna and change in orientation of the distal border of the olecranon process. Based on the present analysis, the origin of the Chaecomysticeti is related to functional changes of the forelimb. Interestingly, the loss of some functions of the forelimb seems to have had a crucial role in the origin of the Chaecomysticeti (see above, Section 3.7. Appendicular skeleton).

Seven morphological transformations are inferred to have been originated at the Balaenomorpha node. These include characters 7, 13, 15, 16, 26, 27 and 28 and represent a major restructuring of the mysticete skeleton. Character 7 is related to the backward position of the nasals (which occurred independently in *Aetiocetus polydentatus*). The transformation related to character 13 consists in a major change in the position of the

orbitotemporal crest that is located on the posterodorsal edge of the supraorbital process of the frontal in nonbalaenomorph mysticetes (and Cetotheriidae), being diagonally oriented from an anteromedial point (lateral to the interorbital region of the frontal) to near the postorbital process of the supraorbital process of the frontal in all the other Balaenomorpha. Additional modifications of the orbitotemporal crest (e.g., the anterior position of this crest in the Balaenopteridae) are not investigated here. The change in the position of the orbitotemporal crest marks a change in the geometry of the temporal muscle, which is probably related to the reduction in the extension of the temporal fossa determined by the shortening and widening of the intertemporal constriction in balaenomorph mysticetes (characters 15 and 16). Characters 26, 27 and 28 describe the reduction in the suprascapular fossa of the scapula, reduction in the greater tubercle and of the deltopectoral crest of the humerus. These characters suggest further functional loss at the level of the forelimb and the possible stabilization of the architecture of the forelimb of the extant mysticetes.

#### 4. Discussion

In recent decades, several works have addressed the early evolution of mysticetes based on new fossil discoveries and new molecular investigations. The morphological analyses of early-diverging mysticetes showed that the assembly of the apomorphic character states of the mysticetes was a gradual process that proceeded step by step with character transformations occurring at different nodes. In particular, Fitzgerald [11] presented an analysis in which step-by-step modifications occurred in different mysticete clades focusing on cranial characters. Our analysis is consistent with that of [11] considering the morphological changes leading up to the balaenomorph characters' appearance in different clades of early, nonbalaenomorph mysticetes. In [11], it was observed that some of the characters that are involved in the bulk feeding in extant mysticetes originated as exaptations in toothed mysticetes, whose functional morphology allows us to conclude they were not bulk feeders. He also suggested that different feeding adaptations occurred independently in nonbalaenomorph mysticetes, uncovering a morphological diversity in the earliest mysticetes suggesting ancient ecological differentiations. A similar conclusion of early trophic niche differentiation in nonbalaenomorph mysticetes was also reached in [89] based on the analysis of size range in Aetiocetidae.

A gradual process of character acquisition in early mysticetes was also proposed in [7] based on morphological and molecular phylogenetic analyses. In that work, the focus was based on the skull characters, and the results show that maxillary and mandibular characters underwent morphological transformations in the earliest-diverging mysticetes.

Most of the published work on the early evolution of mysticetes focused on the origin of characters related to the filter feeding and bulk feeding typical of extant baleen whales. In [7], the presence of palatal foramina and sulci in a toothed aetiocetid whale it is shown, suggesting the coexistence of teeth and baleen in a nonchaemysticete species. This view was challenged [9] by a proposal that suction feeding preceded baleen-assisted feeding in aetiocetids. The morphological characters of the rostrum of *Mystacodon selenensis* were interpreted as indicative of some ability of suction feeding in this early-diverging mysticete [22], somewhat reinforcing the idea expressed in [9] that suction feeding preceded filter feeding in mysticetes. Geisler and coworkers [10], in their analysis of *Coronodon havensteini*, provided a sort of synthetic view suggesting that suction feeding and filter feeding may coexist in a single species as demonstrated by the behaviors of several extant species of marine mammals. However, in their opinion, there is not enough morphological, functional and biometric evidence to support suction feeding in early-diverging, nonbalaenomorph mysticetes.

In a paper dealing with ecomorphological evolution [90], the morphological, developmental and biochemical evidence for a step-wise transition from teeth to baleen was summarized, suggesting that baleen-assisted bulk feeding should be associated with Chaemysticeti based on the reduction of  $C^{13}$  in the bones of these whales, a result related to the transition toward prey on to the lower levels of the food web ([90], p. 1276). This

hypothesis is consistent with the origin of a complete *suite* of morphological adaptations for filter feeding in the earliest chaeomysticete cetaceans, i.e., the Eomysticetidae.

Peredo and coworkers [91] pointed out that the osteological evidence for the presence of baleen is still scanty in taxa in which the full suite of morphological characters present in the rostrum of extant mysticetes is absent. They also suggested that techniques such as the phylogenetic bracket used to infer baleen presence/absence in extinct mysticete clades may be misleading.

Finally, thanks to a study of the neurovascular anatomy of the rostrum of an aetiocetid [8], it was suggested that the distribution and organization of rostral nerves and blood vessels support a hypothesis about the coexistence of teeth and baleen in Aetiocetidae. In that work, a CT scan and 3D imaging were used to reconstruct the anatomy of the neurovascular path in the rostrum of *Aetiocetus weltoni* and provided convincing evidence that the neural and vascular structures related to teeth physiology assisted in the baleen physiology in Aetiocetidae. This kind of anatomical works presents the best evidence to infer the presence of baleen in a nonchaeomysticete taxon, providing strong help in the reconstruction of the transition from teeth to baleen.

Apparently, only a few words have been written about the evolution of the postcranial skeleton during the transition to Mysticeti. In our work, we expand the discussion on the origin of mysticetes by adding data about the morphological changes that occurred in the postcranial skeleton and observing that, like what was observed for the evolution of the rostrum, the postcranial also underwent a step-wise transformation process that led to the characters observed in balaenomorph mysticetes. Based on the distribution of the character states analyzed in the present work, the scapula retained archaeocete-like characteristics in nonbalaenomorph mysticetes and underwent a reduction in the supraspinous fossa in most Balaenomorpha. This reduction is in good agreement with the reduction in the greater tubercle and that in the deltopectoral crest of the humerus in Balaenomorpha, supporting a view of functional loss of motional abilities of the forelimb at the transition from nonbalaenomorph to balaenomorph mysticetes. Similar results were described in [12] in an analysis of postcranial evolution in Neoceti. Their analysis focused on characters of the humerus and vertebrae but did not take into account the scapula, radius and ulna. From our analysis, we observed that the loss of the radial crest of the radius in Eomysticetidae and the coexistence of balaenomorph and nonbalaenomorph characters in the scapulae of *Sitsqwayk cornishorum* and *Horopeta umarere* are suggestive of a step-wise transformation process of the mysticete forelimb rather than a punctuated event, as suggested by the phylogeny of [12]. Additional evolutionary considerations based on the development and evolution of the hindlimb are provided in [92], suggesting that a macroevolutionary event was responsible for the loss of differentiation of lumbar, sacral and caudal vertebrae in the common ancestor of Neoceti together with the loss of the hindlimb patterning system. Additional discussion on this point should be carried out in the context of mysticete vertebral evolution, which is beyond the scope of the present paper.

## 5. Conclusions

The analysis of the mysticete and archaeocete craniomandibular, tympanic and appendicular skeleton supports the hypothesis of a step-wise transition from advanced archaeocetes to mysticetes. The early evolution of mysticetes was characterized by the retention of several archaeocete characters in different skeletal districts (e.g., tympanic bulla, scapula and humerus). Morphological changes are observed in those districts only in later-diverging mysticetes. Nonbalaenomorph mysticetes are characterized by a number of typical mysticete characters in the rostrum (lateral process, infraorbital process, thin lateral edge, multiple dorsal infraorbital foramina and mesorostral groove); these characters coexisted with the presence of archaeocete-like morphologies in the dentary and postcranial skeleton. A number of morphological changes is observed in nonchaeomysticete cetaceans, including the Aetiocetidae, *Maiabalaena* and *Mystacodon*. These include the elongation of the dentary ramus in *Mystacodon* and *Maiabalaena*, the origin of a symphyseal groove

for the mental ligament in the dentary of the Aetiocetidae and the loss of the radial crest. Major morphological changes are then observed in the Balaenomorpha with involvement of the whole skeleton and the final assembly of the structural plan of the mysticete forelimb together with the stabilization of baleen-assisted bulk feeding.

The earliest mysticetes most likely looked different from the extant large and slow whales. They fed and swam in different ways, and their size was not as gigantic as that of the living species. The modifications of the archaic *bauplan* of the earliest-diverging mysticetes occurred in a step-wise transformation process that led to the origin of the architecture of the extant mysticetes, taking place over several millions of years. A large amount of anatomical and comparative work is still necessary to disentangle this transformation path and divide it into smaller steps. We feel that the discovery of new fossil materials is the key to understanding this gradual accumulation of morphological transformation and the origin of the modern-day, giant, baleen-bearing whales.

**Author Contributions:** Conceptualization, M.B. and G.C.; methodology, M.B.; software, M.B.; validation, M.B. and G.C.; formal analysis, M.B.; investigation, M.B.; resources, G.C.; data curation, M.B.; writing—original draft preparation, M.B.; writing—review and editing, M.B. and G.C.; visualization, M.B. and G.C. All authors have read and agreed to the published version of the manuscript.

**Funding:** This research was funded by grants (ex-60%, 2021) from the University of Turin to G.C.

**Institutional Review Board Statement:** Not applicable.

**Data Availability Statement:** All the data used in the present paper are published in the paper.

**Acknowledgments:** We want to express our gratitude to an anonymous reviewer and to Toshiyuki Kimura, who carefully reviewed the manuscript and provided constructive comments that greatly improved the quality and the clarity of this paper. We thank Eric Buffetaut for his highly valuable editorial work. Over the years, discussions with the late Albert Sanders, Thomas A. Deméré and Olivier Lambert have provided us with concepts and ideas that were of help in different moments during the preparation of this article. This work was supported by grants (ex-60%, 2021) from the Università degli Studi di Torino to GC.

**Conflicts of Interest:** The authors declare no conflict of interest.

## References

- Bannister, J.D. Baleen whales. In *Encyclopedia of Marine Mammals*; Perrin, W.F., Würsig, B., Thewissen, J.G.M., Eds.; Academic Press: New York, NY, USA, 2002; pp. 62–72.
- Savoca, M.S.; Czapanskiy, M.F.; Kahane-Rapport, S.R.; Gough, W.T.; Fahlbusch, J.A.; Bierlich, K.C.; Segre, P.S.; Di Clemente, J.; Penry, G.S.; Wiley, D.N.; et al. Baleen whale prey consumption based on high-resolution foraging measurements. *Nature* **2021**, *599*, 85–90. [[CrossRef](#)] [[PubMed](#)]
- Pershing, A.J.; Christensen, L.B.; Record, N.R.; Sherwood, G.D.; Stetson, P.B. The impact of whaling on the ocean carbon cycle: Why bigger was better. *PLoS ONE* **2010**, *5*, e12444. [[CrossRef](#)] [[PubMed](#)]
- Pershing, A.J.; Stamieszkin, K. The North Atlantic ecosystem, from plankton to whales. *Annu. Rev. Mar. Sci.* **2020**, *12*, 339–359. [[CrossRef](#)]
- Sanderson, L.R.; Wassersug, R. Convergent and alternative designs for vertebrate suspension feeding. In *The Skull. Functional and Evolutionary Mechanisms*; Hanken, J., Hall, B.K., Eds.; University of Chicago Press: Chicago, IL, USA, 1993; Volume 3, pp. 37–112.
- Werth, A.J. Feeding in marine mammals. In *Feeding: Form, Function and Evolution in Tetrapod Vertebrates*; Schwenk, K., Ed.; Academic Press: New York, NY, USA, 2000; pp. 475–514.
- Deméré, T.A.; McGowen, M.R.; Berta, A.; Gatesy, J. Morphological and molecular evidence for a stepwise evolutionary transition from teeth to baleen in mysticete whales. *Syst. Biol.* **2008**, *57*, 15–37. [[CrossRef](#)] [[PubMed](#)]
- Ekdale, E.G.; Deméré, T.A. Neurovascular evidence for a co-occurrence of teeth and baleen in an Oligocene mysticete and the transition to filter-feeding in baleen whales. *Zool. J. Linn. Soc.* **2021**, *194*, 395–415. [[CrossRef](#)]
- Marx, F.D.; Hocking, D.P.; Park, T.; Ziegler, T.; Evans, A.R.; Fitzgerald, E.M.G. Suction feeding preceded filtering in baleen whale evolution. *Mem. Mus. Vic.* **2016**, *75*, 71–82. [[CrossRef](#)]
- Geisler, J.H.; Boessenecker, R.W.; Brown, M.; Beatty, B.L. The origin of filter feeding in whales. *Curr. Biol.* **2017**, *27*, 2036–2042.e2. [[CrossRef](#)]
- Fitzgerald, E.M.G. The morphology and systematic of *Mammalodon colliveri* (Cetacea: Mysticeti), a toothed mysticete from the Oligocene of Australia. *Zool. J. Linn. Soc.* **2010**, *158*, 367–476. [[CrossRef](#)]

12. Boessenecker, R.W.; Churchill, M.; Buchholtz, E.A.; Beatty, B.L.; Geisler, J.H. Convergent Evolution of Swimming Adaptations in Modern Whales Revealed by a Large Macrophagous Dolphin from the Oligocene of South Carolina. *Curr. Biol.* **2020**, *30*, 3267–3273.e2. [[CrossRef](#)]
13. Cooper, L.N.; Berta, A.; Dawson, S.D.; Reidenberg, J.S. Evolution of hyperphalangy and digit reduction in the cetacean manus. *Anat. Rec.* **2007**, *290*, 654–672. [[CrossRef](#)]
14. Benke, H. Investigations on the osteology and the functional morphology of the flipper of whales and dolphins (Cetacea). *Investig. Cetacea* **1993**, *24*, 9–252.
15. Mitchell, E.D. A new cetacean from the late Eocene La Meseta Formation, Seymour Island, Antarctic Peninsula. *Can. J. Fish. Aquat. Sci.* **1989**, *46*, 2219–2235. [[CrossRef](#)]
16. Geisler, J.H.; Sanders, A.E. Morphological evidence for the phylogeny of Cetacea. *J. Mamm. Evol.* **2003**, *10*, 23–129. [[CrossRef](#)]
17. Bisconti, M.; Pellegrino, L.; Carnevale, G. Evolution of gigantism in right and bowhead whales (Cetacea: Mysticeti: Balaenidae). *Biol. J. Linn. Soc.* **2021**, *134*, 498–524. [[CrossRef](#)]
18. Bisconti, M.; Damarco, P.; Mao, S.; Pavia, M.; Carnevale, G. The earliest baleen whale from the Mediterranean: Large-scale implications of an early Miocene thalassotherian mysticete from Piedmont, Italy. *Pap. Palaeontol.* **2021**, *7*, 1147–1166. [[CrossRef](#)]
19. Bisconti, M.; Bosselaers, M. A new balaenopterid species from the southern North Sea Basin informs about phylogeny and taxonomy of *Burtinopsis* and *Protororqualus* (Cetacea, Mysticeti, Balaenopteridae). *PeerJ* **2020**, *8*, e9570. [[CrossRef](#)]
20. Tsai, C.-H.; Fordyce, R.E. A new archaic baleen whale *Toipahautea waitaki* (early Late Oligocene, New Zealand) and the origins of crown Mysticeti. *R. Soc. Open Sci.* **2018**, *5*, 172453. [[CrossRef](#)]
21. Peredo, C.M.; Pyenson, N.D.; Marshall, C.D.; Uhen, M.D. Tooth loss precedes the origin of baleen in whales. *Curr. Biol.* **2018**, *28*, 3992–4000.e2. [[CrossRef](#)]
22. de Muizon, C.; Bianucci, G.; Martínez-Cáceres, M.; Lambert, O. *Mystacodon selenensis*, the earliest known toothed mysticete (Cetacea, Mammalia) from the late Eocene of Peru: Anatomy, phylogeny, and feeding adaptations. *Geodiversitas* **2019**, *41*, 401–499. [[CrossRef](#)]
23. Fordyce, R.E.; Marx, F.G. Gigantism precedes filter feeding in baleen whale evolution. *Curr. Biol.* **2018**, *28*, 1670–1676.e2. [[CrossRef](#)]
24. Mead, J.G.; Fordyce, R.E. The therian skull: A lexicon with emphasis on the odontocetes. *Smiths. Contrib. Zool.* **2009**, *627*, 1–216. [[CrossRef](#)]
25. Bisconti, M.; Varola, A. The oldest eschrichtiid mysticete and a new morphological diagnosis of Eschrichtiidae (gray whales). *Riv. It. Paleontol. Strat.* **2006**, *112*, 447–457.
26. Ekdale, E.G.; Berta, A.; Deméré, T.A. The comparative osteology of the petrotympanic complex (ear region) of extant baleen whales (Cetacea: Mysticeti). *PLoS ONE* **2011**, *6*, e21311. [[CrossRef](#)] [[PubMed](#)]
27. Uhen, M.D. Form, function, and anatomy of *Dorudon atrox* (Mammalia, Cetacea): An archaeocete from the middle to late Eocene of Egypt. *Univ. Michigan P. Palaeont.* **2004**, *34*, 1–238.
28. True, F.W. The whalebone whales of the western North Atlantic. *Smiths. Contrib. Knowl.* **1904**, *33*, 1–322.
29. Kellogg, R. Fossil marine mammals from the Miocene Calvert Formation of Maryland and Virginia. *US Natl. Mus. Bull.* **1968**, *247*, 103–197.
30. Bisconti, M.; Damarco, P.; Pavia, M.; Sorce, B.; Carnevale, G. *Marzanoptera tersillae*, a new balaenopterid genus and species from the Pliocene of Piedmont, north-west Italy. *Zool. J. Linn. Soc.* **2021**, *192*, 1253–1292. [[CrossRef](#)]
31. Bisconti, M.; Munsterman, D.K.; Post, K. A new balaenopterid whale from the late Miocene of the Southern North Sea Basin and the evolution of balaenopterid diversity (Cetacea, Mysticeti). *PeerJ* **2019**, *7*, e6915. [[CrossRef](#)]
32. Bisconti, M.; Munsterman, D.K.; Fraaije, R.H.B.; Bosselaers, M.E.J.; Post, K. A new species of rorqual whale (Cetacea, Mysticeti, Balaenopteridae) from the late Miocene of the Southern North Sea Basin and the role of the North Atlantic in the paleobiogeography of *Archaeobalaenoptera*. *PeerJ* **2020**, *8*, e8315. [[CrossRef](#)] [[PubMed](#)]
33. Bisconti, M.; Bosselaers, M. *Fragilicetus velponi*: A new mysticete genus and species and its implications for the origin of Balaenopteridae (Mammalia, Cetacea, Mysticeti). *Zool. J. Linn. Soc.* **2016**, *177*, 450–474. [[CrossRef](#)]
34. Marx, F.G.; Post, K.; Bosselaers, M.; Munsterman, D. A large Late Miocene cetotheriid (Cetacea, Mysticeti) from the Netherlands clarifies the status of *Tranatotcetidae*. *PeerJ* **2019**, *7*, e6426. [[CrossRef](#)] [[PubMed](#)]
35. Peredo, C.M.; Uhen, M.D. A new basal Chaemysticete (Mammalia: Cetacea) from the Oligocene Pysht Formation of Washington, USA. *Pap. Palaeontol.* **2016**, *2016*, 533–554. [[CrossRef](#)]
36. El Adli, J.J.; Deméré, T.A.; Boessenecker, R.W. *Herpetocetus morrowi* (Cetacea: Mysticeti), a new species of diminutive baleen whale from the Upper Pliocene (Piacenzian) of California, USA, with observations on the evolution and relationships of the Cetotheriidae. *Zool. J. Linn. Soc.* **2014**, *170*, 400–466. [[CrossRef](#)]
37. Geisler, J.H.; McGowen, M.R.; Yang, G.; Gatesy, J. A supermatrix analysis of genomic, morphological, and paleontological data from crown Cetacea. *BMC Evol. Biol.* **2011**, *11*, 112. [[CrossRef](#)] [[PubMed](#)]
38. Marx, F.G. The more the merrier? A large cladistic analysis of mysticetes, and comments on the transition from teeth to baleen. *J. Mamm. Evol.* **2011**, *18*, 77–100. [[CrossRef](#)]
39. Deméré, T.A.; Berta, A.; McGowen, M.R. The taxonomic and evolutionary history of fossil and modern balaenopteroid mysticetes. *J. Mamm. Evol.* **2005**, *2*, 99–143. [[CrossRef](#)]

40. Boessenecker, R.W.; Fordyce, R.E. A new eomysticetid from the Oligocene Kokoamu Greensand of New Zealand and a review of the Eomysticetidae (Mammalia, Cetacea). *J. Syst. Palaeontol.* **2016**, *15*, 429–469. [[CrossRef](#)]
41. Boessenecker, R.W.; Fordyce, R.E. A new genus and species of eomysticetid (Cetacea: Mysticeti) and a reinterpretation of “*Mauicetus*” *lophocephalus* Marples, 1956: Transitional baleen whales from the upper Oligocene of New Zealand. *Zool. J. Linn. Soc.* **2015**, *175*, 607–660. [[CrossRef](#)]
42. Boessenecker, R.W.; Fordyce, R.E. Anatomy, feeding ecology, and ontogeny of a transitional baleen whale: A new genus and species of Eomysticetidae (Mammalia: Cetacea) from the Oligocene of New Zealand. *PeerJ* **2015**, *3*, e1129. [[CrossRef](#)]
43. Bisconti, M. Comparative osteology and phylogenetic relationships of *Miocaperea pulchra*, the first fossil pygmy right whale genus and species (Cetacea, Mysticeti, Neobalaenidae). *Zool. J. Linn. Soc.* **2012**, *166*, 876–911. [[CrossRef](#)]
44. Bisconti, M. Skull morphology and phylogenetic relationships of a new diminutive balaenid from the lower Pliocene of Belgium. *Palaeontology* **2005**, *48*, 793–816. [[CrossRef](#)]
45. Churchill, M.; Berta, A.; Deméré, T.D. The systematics of right whales (Mysticeti: Balaenidae). *Mar. Mamm. Sci.* **2012**, *28*, 497–521. [[CrossRef](#)]
46. Kimura, T.; Hasegawa, Y. A new baleen whale (Mysticeti: Cetotheriidae) from the earliest late miocene of Japan and a reconsideration of the phylogeny of cetotheres. *J. Vert. Paleontol.* **2010**, *30*, 577–591. [[CrossRef](#)]
47. Tanaka, Y.; Furusawa, H.; Kimura, M. A new member of fossil balaenid (Mysticeti, Cetacea) from the early Pliocene of Hokkaido, Japan. *R. Soc. Open Sci.* **2020**, *7*, 192182. [[CrossRef](#)]
48. Maddison, W.; Maddison, W.; Mesquite: A Modular System for Evolutionary Analysis. Version: 3.61. 2019. Available online: <http://www.mesquiteproject.org> (accessed on 12 May 2020).
49. Bisconti, M.; Damarco, P.; Tartarelli, G.; Pavia, M.; Carnevale, G. A natural endocast of an early Miocene odontocete and its implications in cetacean brain evolution. *J. Comp. Neurol.* **2021**, *529*, 1198–1227. [[CrossRef](#)]
50. Bisconti, M.; Daniello, R.; Damarco, P.; Tartarelli, G.; Pavia, M.; Carnevale, G. High encephalization in a fossil rorqual illuminates baleen whale brain evolution. *Br. Behav. Evol.* **2021**, *96*, 78–90. [[CrossRef](#)]
51. Bisconti, M. Evolutionary history of Balaenidae. *Cranium* **2003**, *20*, 9–50.
52. McLeod, S.A.; Whitmore, F.C., Jr.; Barnes, L.G. Evolutionary relationships and classification. In *The Bowhead Whale*; Burns, J.J., Montague, J.J., Cowles, C.J., Eds.; Society for Marine Mammalogy: Yarmouth Port, MA, USA, 1993; Volume 2, pp. 45–70.
53. Bisconti, M. Anatomy of a new cetotheriid genus and species from the Miocene of Herentals, Belgium, and the phylogenetic and paleobiogeographic relationships of Cetotheriidae s.s. (Mammalia, Cetacea, Mysticeti). *J. Syst. Palaeontol.* **2015**, *13*, 377–395. [[CrossRef](#)]
54. Bouetel, V.; de Muizon, C. The anatomy and relationships of *Piscobalaena nana* (Cetacea, Mysticeti), a Cetotheriidae s.s. from the early Pliocene of Peru. *Geodiversitas* **2006**, *28*, 319–395.
55. Hanna, G.D.; McLellan, M. A new species of whale from the type locality of the Monterey Group. *Proc. Calif. Acad. Sci.* **1924**, *13*, 237–241.
56. Kellogg, R. The history of whales—Their adaptation to life in the water. *Q. Rev. Biol.* **1928**, *3*, 29–76. [[CrossRef](#)]
57. Portis, A. Catalogo descrittivo dei Talassoterii rinvenuti nei terreni terziari del Piemonte e della Liguria. *Mem. R. Acc. Sci. Torino* **1884**, *37*, 247–365.
58. Bisconti, M. A new basal balaenopterid from the Early Pliocene of northern Italy. *Palaeontology* **2007**, *50*, 1103–1122. [[CrossRef](#)]
59. Bisconti, M.; Ochoa, D.; Urbina, M.; Salas-Gismondi, R. *Archaeobalaenoptera eusebioi*, a new rorqual from the late Miocene of Peru (Cetacea, Mysticeti, Balaenopteridae) and its impact in reconstructing body size evolution, ecomorphology and paleobiogeography of Balaenopteridae. *J. Syst. Palaeontol.* **2022**, *in press*. [[CrossRef](#)]
60. Zeigler, C.V.; Chan, G.L.; Barnes, L.G. A new Late Miocene balaenopterid whale (Cetacea: Mysticeti), *Parabalaenoptera baulinensis*, (new genus and species) from the Santa Cruz Mudstone, Point Reyes Peninsula, California. *Proc. Calif. Acad. Sci. USA* **1997**, *50*, 115–138.
61. Gol’Din, P.; Steeman, M.E. From problem taxa to problem solver: A new Miocene family, Tranatocetidae, brings perspective on baleen whale evolution. *PLoS ONE* **2015**, *10*, e0135500. [[CrossRef](#)] [[PubMed](#)]
62. Wada, S.; Oishi, M.; Yamada, T.K. A newly discovered species of living baleen whale. *Nature* **2003**, *426*, 278–281. [[CrossRef](#)]
63. Miller, G.S. The telescoping of the cetacean skull. *Smiths. Misc. Coll.* **1923**, *76*, 1–70.
64. Roston, R.A.; Roth, V.L. Cetacean Skull Telescoping Brings Evolution of Cranial Sutures into Focus. *Anat. Rec.* **2019**, *302*, 1055–1073. [[CrossRef](#)]
65. Marx, F.G.; Fordyce, R.E. A link no longer missing: New evidence for the cetotheriid affinities of *Caperea*. *PLoS ONE* **2016**, *11*, e0164059. [[CrossRef](#)] [[PubMed](#)]
66. Bueno, M.R.; Fernández, M.S.; Cozzuol, M.A.; Cuitiño, J.I.; Fitzgerald, E.M.G. The early Miocene balaenid *Morenocetus parvus* from Patagonia (Argentina) and the evolution of right whales. *PeerJ* **2018**, *5*, e4148. [[CrossRef](#)] [[PubMed](#)]
67. Tsai, C.-H.; Fordyce, R.E. Disparate heterochronic processes in baleen whale evolution. *Evol. Biol.* **2014**, *41*, 299–307. [[CrossRef](#)]
68. Kellogg, R. A review of the Archaeoceti. *Carnegie Inst. Wash. Publ.* **1936**, *482*, 1–455.
69. Gol’Din, P.; Startsev, D. *Brandtocetus*, a new genus of baleen whales (Cetacea, Cetotheriidae) from the late Miocene of Crimea, Ukraine. *J. Vert. Paleontol.* **2014**, *34*, 419–433. [[CrossRef](#)]
70. Kellogg, R. A new whalebone whale from the Miocene Calvert Formation. *US Natl. Mus. Bull.* **1965**, *247*, 1–45.

71. Ritsche, I.S.; Fahlke, J.M.; Wieder, F.; Hilger, A.; Manke, I.; Hampe, O. Relationships of cochlear coiling shape and hearing frequencies in cetaceans, and the occurrence of infrasonic hearing in Miocene Mysticeti. *Foss. Rec.* **2018**, *21*, 33–45. [[CrossRef](#)]
72. Park, T.; Evans, A.R.; Gallagher, S.J.; Fitzgerald, E.M.G. Low-frequency hearing preceded the evolution of giant body size and filter feeding in baleen whales. *Proc. R. Soc. B* **2017**, *284*, 20162528. [[CrossRef](#)]
73. Ekdale, E.G. Morphological Variation Among the Inner Ears of Extinct and Extant Baleen Whales (Cetacea: Mysticeti). *J. Morphol.* **2016**, *277*, 1599–1615. [[CrossRef](#)]
74. Shadwick, R.E.; Goldbogen, J.A.; Pyenson, N.D.; Whale, J.C.A. Structure and function in the lunge feeding apparatus: Mechanical properties of the fin whale mandible. *Anat. Rec.* **2017**, *300*, 1953–1962. [[CrossRef](#)]
75. Pyenson, N.D.; Goldbogen, J.A.; Shadwick, R.E. Mandible allometry in extant and fossil Balaenopteridae (Cetacea: Mammalia): The largest vertebrate skeletal element and its role in rorqual lunge feeding. *Biol. J. Linn. Soc.* **2013**, *108*, 586–599. [[CrossRef](#)]
76. Pyenson, N.D.; Sponberg, S.N. Reconstructing body size in extinct crown Cetacea (Neoceti) using allometry, phylogenetic methods and tests from the fossil record. *J. Mamm. Evol.* **2011**, *18*, 269–288. [[CrossRef](#)]
77. Kimura, T. Feeding strategy of an early Miocene cetother from the Toyama and Akeyo Formations, central Japan. *Paleontol. Res.* **2002**, *6*, 179–189.
78. Bisconti, M. New description, character analysis and preliminary phyletic assessment of two Balaenidae skulls from the Italian Pliocene. *Palaeontogr. Ital.* **2000**, *87*, 37–66.
79. Lambertsen, R.H. Internal mechanism of rorqual feeding. *J. Mamm.* **1983**, *64*, 76–88. [[CrossRef](#)]
80. Gol'Din, P.; Startsev, D.; Krakhmalnaya, T. The anatomy of the late Miocene baleen whale *Cetotherium riabinini* from Ukraine. *Acta Palaeontol. Pol.* **2014**, *59*, 795–814.
81. Steeman, M.E. A new baleen whale from the late Miocene of Denmark and early mysticete hearing. *Palaeontology* **2009**, *52*, 1169–1190. [[CrossRef](#)]
82. Lambertsen, R.H.; Ulrich, N.; Straley, J. Frontomandibular stay of Balaenopteridae: A mechanism for momentum recapture during feeding. *J. Mamm.* **1995**, *76*, 877–899. [[CrossRef](#)]
83. Bisconti, M. Taxonomic revision and phylogenetic relationships of the rorqual-like mysticete from the Pliocene of Mount Pulgnasco, northern Italy (Mammalia, Cetacea, Mysticeti). *Palaeontogr. Ital.* **2007**, *91*, 85–108.
84. Gillet, A.; Frédéric, B.; Parmentier, E. Divergent evolutionary morphology of the axial skeleton as a potential key innovation in modern cetaceans. *Proc. R. Soc. B* **2019**, *286*, 20191771. [[CrossRef](#)]
85. Buchholtz, E.A. Vertebral and rib anatomy in *Caperea marginata*: Implications for evolutionary patterning of the mammalian vertebral column. *Mar. Mamm. Sci.* **2011**, *27*, 382–397. [[CrossRef](#)]
86. Buchholtz, E.A. Modular evolution of the cetacean vertebral column. *Evol. Dev.* **2007**, *9*, 278–289. [[CrossRef](#)] [[PubMed](#)]
87. Buchholtz, E.A. Implications of vertebral morphology for locomotor evolution in early Cetacea. In *The Emergence of Whales*; Thewissen, J.G.M., Ed.; Plenum Press: New York, NY, USA, 1998; pp. 325–351.
88. Duboys de Lavigerie, G.; Bosselaers, M.; Goolaerts, S.; Park, T.; Lambert, O.; Marx, F.G. New Pliocene right whale from Belgium informs balaenid phylogeny and function. *J. Syst. Palaeontol.* **2020**, *18*, 1141–1166. [[CrossRef](#)]
89. Tsai, C.-H.; Ando, T. Niche partitioning in Oligocene toothed mysticetes (Mysticeti: Aetiocetidae). *J. Mamm. Evol.* **2016**, *23*, 33–41. [[CrossRef](#)]
90. Berta, A.; Lanzetti, A.; Ekdale, E.G.; Deméré, T.A. From teeth to baleen and raptorial to bulk filter feeding in mysticete cetaceans: The role of paleontological, genetic, and geochemical data in feeding evolution and ecology. *Integr. Comp. Biol.* **2016**, *56*, 1271–1284. [[CrossRef](#)] [[PubMed](#)]
91. Peredo, C.M.; Pyenson, N.D.; Uhen, M.D.; Marshall, C.D. Alveoli, teeth, and tooth loss: Understanding the homology of internal mandibular structures in mysticete cetaceans. *PLoS ONE* **2017**, *12*, e0178243. [[CrossRef](#)]
92. Thewissen, J.G.M.; Cohn, M.J.; Stevens, L.S.; Bajpai, S.; Heyning, J.; Horton, W.E., Jr. Developmental basis for hind-limb loss in dolphins and origin of the cetacean bodyplan. *Proc. Natl. Acad. Sci. USA* **2006**, *103*, 8414–8418. [[CrossRef](#)] [[PubMed](#)]